

1164-10-10
TMX-51072

MTP-AERO-63-60

July 1, 1963

33

GEORGE C. MARSHALL

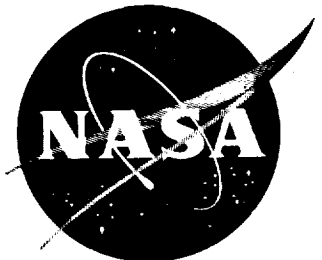
**SPACE
FLIGHT
CENTER**

HUNTSVILLE, ALABAMA

AN EVALUATION OF VARIOUS GEOMAGNETIC
FIELD EQUATIONS

By

Harold C. Euler and Peter E. Wasko



FOR INTERNAL USE ONLY

NAUTICS AND SPACE ADMINISTRATION

1

2

3

4

5

6

7

8

9

10

11

12

GEORGE C. MARSHALL SPACE FLIGHT CENTER

MTP -AERO-63-60

AN EVALUATION OF VARIOUS GEOMAGNETIC
FIELD EQUATIONS

By

Harold C. Euler and Peter E. Wasko

ABSTRACT

The dipole and multipole approximations of the Earth's main magnetic field are evaluated using Jensen and Whitaker's 568 Gaussian coefficients for Epoch 1955.0. The total geomagnetic field, which was computed to 16 earth radii for various geographic locations, is compared to values computed with the inverse cube law and to some of the Vanguard III geomagnetic field observations.

1

2

3

4

5

6

GEORGE C. MARSHALL SPACE FLIGHT CENTER

MTP-AERO-63-60

July 1, 1963

AN EVALUATION OF VARIOUS GEOMAGNETIC
FIELD EQUATIONS

By

Harold C. Euler and Peter E. Wasko

SPACE ENVIRONMENT SECTION
AEROPHYSICS AND ASTROPHYSICS BRANCH
AEROBALLISTICS DIVISION

TABLE OF CONTENTS

	Page
I. INTRODUCTION.....	2
II. GEOMAGNETIC FIELD EQUATIONS.....	3
A. Spherical Harmonic Analysis of the Main Field	3
1. The Geomagnetic Field Equation.....	3
2. The Schmidt Normalized Legendre Function in... the Geomagnetic Potential Equation	4
3. The Gaussian Coefficients in the Geomagnetic.... Potential Equation	7
4. The Radius-ratio Factor in Equation 2	7
B. Inverse Cube Analysis of the Main Field	8
III. EVALUATION PROCEDURES.....	8
IV. PRESENTATION AND DISCUSSION OF THE RESULTS...	9
V. CONCLUSIONS.....	11

LIST OF ILLUSTRATIONS

Figure	Title	Page
1.	Jensen and Whitaker's Normalized Gaussian Coefficients, Epoch 1955.0	16
2.	Normalizing Factor, C_n^m	17
3.	Jensen and Whitaker's Unnormalized Gaussian Coefficients	18
4. a.	Plot of Some Unnormalized Gaussian Coefficients, g_n^m , from Epochs 1835-1955	19
4. b.	Plot of Some Unnormalized Gaussian Coefficients, h_n^m , from Epochs 1835-1955	20
5.	Radius-Ratio Factor for Various Degrees, n	21
6.	Total Geomagnetic Field for Various S - Truncation Levels and for the Inverse Cube Relation for Colatitude $\theta = 60^\circ$, Longitude East $\lambda = 280^\circ$	22
7. a.	Total Geomagnetic Field at Various Altitudes above the Earth's Surface for 30° Colatitude, 280° Longitude. The arrows and corresponding numbers identify the percent truncation levels	23
7. b.	Total Geomagnetic Field at Various Altitudes above the Earth's Surface for 30° Colatitude, 280° Longitude	24
8. a.	Total Geomagnetic Field at Various Altitudes above the Earth's Surface for 60° Colatitude, 280° Longitude. The arrows and corresponding numbers identify the percent truncation levels	25
8. b.	Total Geomagnetic Field at Various Altitudes above the Earth's Surface for 60° Colatitude, 280° Longitude. The arrows and corresponding numbers identify the percent truncation levels	26

LIST OF ILLUSTRATIONS (CONTD)

Figure	Title	Page
8. c.	Total Geomagnetic Field at Various Altitudes above the Earth's Surface for 60° Colatitude, 280°E Longitude	27
9. a.	Total Geomagnetic Field at Various Altitudes above the Earth's Surface for 89° Colatitude, 280°E Longitude. The arrows and corresponding numbers identify the percent truncation levels	28
9. b.	Total Geomagnetic Field at Various Altitudes above the Earth's Surface for 89° Colatitude, 280°E Longitude	29
10. a.	Cross section of the number of Legendre polynomials necessary to attain the truncation level of $\pm 3\%$ difference from the total geomagnetic field value computed with 296 Legendre polynomials. Jensen and Whitaker's 568 Gaussian coefficients ($1 \leq n \leq 24$; $0 \leq m \leq 17$) for Epoch 1955.0 were used. The isolines are labeled in units of number of Legendre polynomials, S	30
10. b.	Cross section of the number of Legendre polynomials necessary to attain the truncation level of $\pm 2\%$ difference from the total geomagnetic field value computed with 296 Legendre polynomials. Jensen and Whitaker's 568 Gaussian coefficients ($1 \leq n \leq 24$; $0 \leq m \leq 17$) for Epoch 1955.0 were used. The isolines are labeled in units of number of Legendre polynomials, S	31
10. c.	Cross section of the number of Legendre polynomials necessary to attain the truncation level of $\pm 1\%$ difference from the total geomagnetic field value computed with 296 Legendre polynomials. Jensen and Whitaker's 568 Gaussian coefficients ($1 \leq n \leq 24$; $0 \leq m \leq 17$) for Epoch 1955.0 were used. The isolines are labeled in units of number of Legendre polynomials, S	32

LIST OF ILLUSTRATIONS (CONTD)

Figure	Title	Page
10. d.	Cross section of the number of Legendre polynomials necessary to attain the truncation level of $\pm 0.5\%$ difference from the total geomagnetic field value computed with 296 Legendre polynomials. Jensen and Whitaker's 568 Gaussian coefficients ($1 \leq n \leq 24$; $0 \leq m \leq 17$) for Epoch 1955.0 were used. The isolines are labeled in units of number of Legendre polynomials, S	33
10. e.	Cross section of the number of Legendre polynomials necessary to attain the truncation level of $\pm 0.1\%$ difference from the total geomagnetic field value computed with 296 Legendre polynomials. Jensen and Whitaker's 568 Gaussian coefficients ($1 \leq n \leq 24$; $0 \leq m \leq 17$) for Epoch 1955.0 were used. The isolines are labeled in units of number of Legendre polynomials, S	34
11. a.	Cross section of the number of Legendre polynomials necessary to attain the truncation level of $\pm 3\%$ difference from the total geomagnetic field value computed with 296 Legendre polynomials. Jensen and Whitaker's 568 Gaussian coefficients ($1 \leq n \leq 24$; $0 \leq m \leq 17$) for Epoch 1955.0 were used. The isolines are labeled in units of number of Legendre polynomials, S	35
11. b.	Cross section of the number of Legendre polynomials necessary to attain the truncation level of $\pm 2\%$ difference from the total geomagnetic field value computed with 296 Legendre polynomials. Jensen and Whitaker's 568 Gaussian coefficients ($1 \leq n \leq 24$; $0 \leq m \leq 17$) for Epoch 1955.0 were used. The isolines are labeled in units of number of Legendre polynomials, S	36

LIST OF ILLUSTRATIONS (CONTD)

Figure	Title	Page
11. c.	Cross section of the number of Legendre polynomials necessary to attain the truncation level of $\pm 1\%$ difference from the total geomagnetic field value computed with 296 Legendre polynomials. Jensen and Whitaker's 568 Gaussian coefficients ($1 \leq n \leq 24$; $0 \leq m \leq 17$) for Epoch 1955.0 were used. The isolines are labeled in units of number of Legendre polynomials, S	37
11. d.	Cross section of the number of Legendre polynomials necessary to attain the truncation level of $\pm 0.5\%$ difference from the total geomagnetic field value computed with 296 Legendre polynomials. Jensen and Whitaker's 568 Gaussian coefficients ($1 \leq n \leq 24$; $0 \leq m \leq 17$) for Epoch 1955.0 were used. The isolines are labeled in units of number of Legendre polynomials, S	38
11. e.	Cross section of the number of Legendre polynomials necessary to attain the truncation level of $\pm 0.1\%$ difference from the total geomagnetic field value computed with 296 Legendre polynomials. Jensen and Whitaker's 568 Gaussian coefficients ($1 \leq n \leq 24$; $0 \leq m \leq 17$) for Epoch 1955.0 were used. The isolines are labeled in units of number of Legendre polynomials, S	39
12. a.	Cross section of the maximum percent truncation levels for 280° E longitude. The isolines are in percent units	40
12. b.	Cross section of the maximum percent truncation levels for 100° E longitude. The isolines are in percent units	41
12. c.	Cross section of the percent truncation levels at 60° colatitude, 280° E longitude. The isolines are in percent units	42

LIST OF ILLUSTRATIONS (CONTD)

Figure	Title	Page
13. a.	Percent Truncation Levels at Various Colatitudes for $S = 1$	43
13. b.	Percent Truncation Levels at Various Colatitudes for $S = 2$	44
13. c.	Percent Truncation Levels at Various Colatitudes for $S = 3$	45
13. d.	Percent Truncation Levels at Various Colatitudes for $S = 4$	46
13. e.	Percent Truncation Levels at Various Colatitudes for $S = 5$	47
13. f.	Percent Truncation Levels at Various Colatitudes for $S = 10$	48
14.	Percent Deviations at Various Colatitudes of the Geomagnetic Field Computed with the Inverse Cube Relation from that Computed for $S = 296$	49
15.	Percentile Levels of Percent Deviations of the Vanguard III Measured Field from that Computed for $S = 296$	50
16. a.	Mean and Extreme Geomagnetic Field Curves for Epoch 1955.0	51
16. b.	Mean and Extreme Geomagnetic Field Curves for Epoch 1955.0	52

DEFINITION OF SYMBOLS

SYMBOL	DEFINITION
B_L	Total geomagnetic field using the entire 296 Legendre polynomials
B_S	Total geomagnetic field using S Legendre polynomials
C_n^m	Schmidt partially normalizing factor
H	Distance above a 6371.2 km spherical earth
P_n^m	Normalized Legendre function of Schmidt
S	Truncation level in terms of total number of Legendre polynomials arranged in the sequence used by Schmidt
T	Truncation level in terms of percent deviation of B_S from B_L
V	The geomagnetic potential
X	North component of the geomagnetic field
Y	East component of the geomagnetic field
Z	Vertical component of the geomagnetic field
a	Mean radius of earth
m	Order of a polynomial
n	Degree of a polynomial
r	Radial distance from earth's center
θ	Geocentric colatitude
λ	Geocentric east longitude

1. The first part of the document is a list of names.

2. The second part is a list of dates.

3. The third part is a list of times.

4. The fourth part is a list of locations.

5. The fifth part is a list of events.

6. The sixth part is a list of people.

7. The seventh part is a list of places.

8. The eighth part is a list of things.

9. The ninth part is a list of actions.

10. The tenth part is a list of results.

11. The eleventh part is a list of conclusions.

12. The twelfth part is a list of recommendations.

13. The thirteenth part is a list of suggestions.

14. The fourteenth part is a list of notes.

15. The fifteenth part is a list of references.

GEORGE C. MARSHALL SPACE FLIGHT CENTER

MTP-AERO-63-60

AN EVALUATION OF VARIOUS GEOMAGNETIC
FIELD EQUATIONS

By

Harold C. Euler and Peter E. Wasko

SUMMARY

An evaluation of the spherical harmonic fitted geomagnetic field equations using Jensen and Whitaker's coefficients and of the inverse cube geomagnetic field equation is undertaken in this report. The total fields calculated with the former equation are compared with those computed with the latter equation and with Vanguard III field measurements.

The total geomagnetic fields were computed at 0, 100, 200, 300, 400, 600, 800, 1000, 1500, 2000, 3000 and 4000 km and at 1, 2, 4, 8 and 16 earth radii above a 6371.2 km spherical earth for colatitudes 0° , 10° , 15° , 30° , 45° , 60° , 75° , and 89° both at 80° W and 100° E longitudes. For each of these locations the fields were calculated using the Jensen and Whitaker's coefficients for $S = 1, 2, 3, \dots, 296$, where S is the total number of Legendre polynomials arranged in the sequence used by Schmidt. The inverse cube fields were also calculated for these locations. The Vanguard III field measurements used were in the altitude range, 600 - 3800 km, in the geographic area, from 2° to 34° N latitude and from 75° to 83° W longitude.

Various graphs showing the percent truncation levels, S truncation levels, and percent deviations of inverse cube fields and measured fields from the fields computed for $A = 296$ Legendre polynomials were constructed and interpreted.

The most important deductions of the evaluation study are summarized and presented in the section on conclusions.

SECTION I. INTRODUCTION

A determination of the expected geomagnetic field environment is important for input to launch vehicle and spacecraft design and performance studies. Many control features have torque-producing magnetic components which tend to change vehicle spin and orientation. The resultant torque on the spacecraft is equal to the cross product of the spacecraft magnetic moment vector with the total geomagnetic field intensity vector. The geomagnetic field, at the earth's surface, is of the order of magnitude of $1/2$ Gauss varying with latitude and longitude and decreasing with altitude. The vertical extent of the geomagnetosphere, typically about 10^5 km, varies with solar activity which produces solar flare plasmas and changes in the solar wind (Refs. 1 and 2). The geomagnetosphere ranges, in extent, from approximately 8 earth radii on the daytime side of the earth to about 60 earth radii (Ref. 1) on the nighttime side depending upon solar activity.

The inverse cube geomagnetic field equation and a spherical harmonic fitted geomagnetic field equation of various orders and degrees have been used to compute the fields at various altitudes. Jensen and Whitaker produced a spherical harmonic fit to the Epoch 1955.0 surface geomagnetic field to degree 24 and order 17. In this report an evaluation of these two geomagnetic field equations is undertaken by (1) determining the truncation errors due to the omission of higher degree and order Legendre polynomials in the Jensen and Whitaker Epoch 1955.0 spherical harmonic fit to the surface geomagnetic field and (2) comparing the geomagnetic field values computed by the spherical harmonic fitted equation with (a) values computed by the inverse cube law, and (b) some values observed by the Vanguard III Satellite.

Acknowledgements: The authors wish to express their gratitude to Mr. R. W. Murray, Physics Division, Headquarters, Air Force Special Weapons Center, for providing them with a listing of the 704 Subroutine "MAGFLD" and a list of the Jensen and Whitaker's Gaussian coefficients for Epoch 1955.0 and to Mr. J. D. Armstrong, Computation Division, George C. Marshall Space Flight Center, who programmed the geomagnetic field equations on the Burroughs 205 and G.E. 225. Also, the considerable assistance rendered by Mr. F. D'Arcangelo, Mr. T. A. King, and Mr. W. T. Roberts, Space

Environment Section, Aeroballistics Division, George C. Marshall Space Flight Center, in computing and checking data and in plotting the graphs used in this report is gratefully acknowledged. We also would like to thank Dr. Heybey for his extensive review and constructive comments.

SECTION II. GEOMAGNETIC FIELD EQUATIONS

A. SPHERICAL HARMONIC ANALYSIS OF THE MAIN FIELD

1. The Geomagnetic Field Equation. The geomagnetic potential of internal origin (Ref. 3) is expressed as:

$$V = a \sum_{n=1}^k \sum_{m=0}^n \left(\frac{a}{r}\right)^{n+1} (g_n^m \cos m\lambda + h_n^m \sin m\lambda) P_n^m(\cos \theta) \quad (1)$$

where: λ is longitude East
 V is the geomagnetic potential
 θ is the colatitude
 a is the mean radius of the earth
 r is the radial distance from earth's center
 $P_n^m(\cos \theta)$ are Legendre functions
 n refers to the degree of the Legendre polynomial
 m refers to the order of the Legendre polynomial

By differentiating Eq. (1), the geomagnetic field components are:

$$X = \frac{\partial V}{r \partial \theta} = \sum_{n=0}^k \sum_{m=0}^n \left(\frac{a}{r}\right)^{n+2} (g_n^m \cos m\lambda + h_n^m \sin m\lambda) \frac{\partial P_n^m(\cos \theta)}{\partial \theta} \quad (2a)$$

$$Y = -\frac{1}{r \sin \theta} \frac{\partial V}{\partial \lambda} = \sum_{n=0}^k \sum_{m=0}^n \left(\frac{a}{r}\right)^{n+2} \frac{m}{\sin \theta} (g_n^m \sin m\lambda - h_n^m \cos m\lambda) P_n^m(\cos \theta) \quad (2b)$$

$$Z = \frac{\partial V}{\partial r} = - \sum_{n=0}^k \sum_{m=0}^n (n+1) \left(\frac{a}{r}\right)^{n+2} (g_n^m \cos m\lambda + h_n^m \sin m\lambda) P_n^m(\cos \theta) \quad (2c)$$

where (Ref. 2): X is the northward horizontal component
 Y is the eastward horizontal component
 Z is the downward vertical component

The total geomagnetic field is accordingly:

$$B = \sqrt{X^2 + Y^2 + Z^2} \quad (3)$$

2. The Schmidt Normalized Legendre Function in the Geomagnetic Potential Equation. The Schmidt normalized Legendre functions (Ref. 4) can be derived as follows:

$$\begin{aligned} P_n^m(\cos \theta) &= (2 - \delta_m^0) \frac{(n-m)!}{(n+m)!} \left[\frac{1}{2} \right]^{\frac{1}{2}} \sin^m \theta \frac{d^m P_n(\cos \theta)}{d(\cos \theta)^m} = \\ &= \left[(2 - \delta_m^0) \frac{(n-m)!}{(n+m)!} \right]^{\frac{1}{2}} \frac{(2n)!}{2^n n! (n-m)!} \sin^m \theta \left\{ \cos^{n-m} \theta - \right. \\ &\quad - \frac{(n-m)(n-m-1)}{2(2n-1)} \cos^{n-m-2} \theta + \\ &\quad + \frac{(n-m)(n-m-1)(n-m-2)(n-m-3)}{2(4)(2n-1)(2n-3)} \\ &\quad \left. \cos^{n-m-4} \theta - \dots \right\} \quad (4) \end{aligned}$$

where: $m = 0, 1, 2, \dots, n$
 $n = 0, 1, 2, \dots, k$
 $\delta_m^0 = 1$, when $m = 0$ and $\delta_m^0 = 0$, when $m \neq 0$.

An example using Eq. (4) to generate the Legendre polynomials and Eq. (2) to compute the geomagnetic field component contributions, X_n^m , for $n \leq 2$, and $m \leq n$ follows:

Let,

$$u_n^m = \cos^{n-m} \theta - \frac{(n-m)(n-m-1)}{2(2n-1)} \cos^{n-m-2} \theta + \dots \quad (5)$$

and

$$C_n^m = \left[(2 - \delta_m^0) \frac{(n-m)!}{(n+m)!} \right]^{\frac{1}{2}} \frac{(2n)!}{2^n n! (n-m)!} \quad (6)$$

then,

$$P_n^m(\cos \theta) = C_n^m \sin^m \theta u_n^m \quad (7)$$

and,

$$\begin{aligned} \frac{\partial P_n^m(\cos \theta)}{\partial \theta} &= C_n^m \left[\sin^m \theta \frac{\partial u_n^m}{\partial \theta} + \sin^{m-1} \theta u_n^m m \cos \theta \right] = \\ &= C_n^m \sin^m \theta \frac{\partial u_n^m}{\partial \theta} + m \cot \theta P_n^m(\cos \theta) \end{aligned} \quad (8)$$

but,

$$\begin{aligned} \frac{\partial u_n^m}{\partial \theta} &= - (n-m) \cos^{n-m-1} \theta \sin \theta + \frac{(n-m)(n-m-1)(n-m-2)}{2(2n-1)} \\ &\cos^{n-m-3} \theta \sin \theta - \dots \end{aligned} \quad (9)$$

then,

$$\begin{aligned} \frac{\partial P_n^m}{\partial \theta} &= C_n^m \sin^{m+1} \theta \left[- (n-m) \cos^{n-m-1} \theta + \right. \\ &\quad \left. + \frac{(n-m)(n-m-1)(n-m-2)}{2(2n-1)} \cos^{n-m-3} \theta - \dots \right] + \\ &\quad + m \cot \theta P_n^m(\cos \theta) \end{aligned} \quad (10)$$

The P_n^m , $\frac{\partial P_n^m}{\partial \theta}$ and X_n^m expressions derived from Eqs. (4-10) for $1 \leq n \leq 2$ and $0 \leq m \leq n$ are shown in Table I.

Table I

An Example of the Schmidt Normalized Polynomials, P_n^m , and the X_n^m Geomagnetic Field Contributions for $1 \leq n \leq 2$ and $0 \leq m \leq n$

P_n^m	m		
	0	1	2
1	$\cos \theta$	$\sin \theta$	
2	$3/2(\cos^2 \theta - 1/3)$	$\sqrt{3} \sin \theta \cos \theta$	$\frac{\sqrt{3}}{2} \sin^2 \theta$

$\frac{\partial P_n^m}{\partial \theta}$	m		
	0	1	2
1	$-\sin \theta$	$\cos \theta$	
2	$-3 \sin \theta \cos \theta$	$\sqrt{3}(\cos^2 \theta - \sin^2 \theta)$	$\sqrt{3} \sin \theta \cos \theta$

X_n^m	m		
	0	1	2
1	$-\left(\frac{a}{r}\right)^3 (\sin \theta) g_1^0$	$\left(\frac{a}{r}\right)^3 \cos \theta (g_1^1 \cos \lambda + h_1^1 \sin \lambda)$	
2	$-\left(\frac{a}{r}\right)^4 (\sin \theta \cos \theta) g_2^0$	$\left(\frac{a}{r}\right)^4 \sqrt{3} (\cos^2 \theta - \sin^2 \theta) (g_2^1 \cos \lambda + h_2^1 \sin \lambda)$	$\left(\frac{a}{r}\right)^4 \sqrt{3} \sin \theta \cos \theta (g_2^2 \cos 2\lambda + h_2^2 \sin 2\lambda)$

3. The Gaussian Coefficients in the Geomagnetic Potential

Equation. The Gaussian coefficients, g_n^m and h_n^m , in Eq. (1) are interpreted as the Schmidt's Gaussian coefficients used by Vestine (Ref. 5) following Schmidt's introduction of his normalized Legendre functions, P_n^m . The Schmidt's Gaussian coefficients when multiplied by the negative of the normalizing factor C_n^m from Eq. (6) produce the Gaussian coefficients as introduced by Gauss (Ref. 5). The Jensen and Whitaker's coefficients are similar to the Gaussian coefficients used by Gauss. To illustrate the effect of applying the normalizing factor to the Jensen and Whitaker's coefficients, these coefficients were graphed in Fig. 1 to $n = 12$ and $m = 12$ in the sequence used by Schmidt. According to this sequence the abscissas in Figs. 1 - 3 are labeled in Legendre polynomial number. A table is inserted in each figure to identify the polynomial number with its appropriate degree and order and hence with the corresponding degree and order of the Gaussian coefficient and normalizing factor. It can be seen in Fig. 1 that the amplitude of the curves tends to increase markedly with increasing n . The corresponding values of C_n^m are graphed in Fig. 2 in the same sequence as used in Fig. 1; the corresponding Gaussian coefficients are shown in Fig. 3. It can be seen in Figs. 2 and 3 that the amplitude of the normalizing factor increases markedly with n and that the absolute values of the unnormalized Gaussian coefficients decrease markedly with increasing n . It will be noted later that the contributions to the geomagnetic field by higher n -terms also decrease appreciably.

Of interest is the change in values of the lower degree and order unnormalized Gaussian coefficients since Epoch 1835. The values of these Gaussian coefficients (Refs. 5 - 10) are plotted in Fig. 4. The changes in the g - and h -coefficients are probably due to such factors as: (1) the total number of points and geographic area used in the curve fit, (2) the number of coefficients used to fit the data, (3) a real secular trend, and (4) instrument accuracy.

4. The Radius-ratio Factor in Equation 2. The radius-ratio factor $\left(\frac{a}{r}\right)^{n+2}$, where " a " is the mean radius of the earth and " r " is the radial distance from the earth's center through the surface geographic point to the altitude desired above the earth's surface, is graphed in Fig. 5. It can be seen that this factor decreases rapidly with altitude and increasing " n ".

B. INVERSE CUBE ANALYSIS OF THE MAIN FIELD

According to the inverse cube geomagnetic field equation, the geomagnetic field, B_h , at any altitude, h , above the earth's surface is

$$B_h = B_0 \left(\frac{a}{r} \right)^3$$

where " B_0 " is the surface geomagnetic field, " a " is the mean earth's radius, and " r " is the radial distance from the earth's center.

SECTION III. EVALUATION PROCEDURES

A. The procedure of evaluating the contribution of higher degree and order polynomials in Eq. (2) to the total geomagnetic field in Eq. (3) is based on the following percent deviation expression:

$$\frac{B_S - B_L}{B_L} \times 100\%$$

where B_L is the total geomagnetic field using all of the Jensen and Whitaker's coefficients (to $n = 24$, $m = 17$) and B_S is the field value at some truncation level, S , where $n < 24$ and $m \leq 17$, of the series in Eq. (2). The truncation level can be identified either in terms of the percent deviation, T , of B_S from B_L or in terms of the total number, S , of Legendre polynomials in the Schmidt's sequence (see table inserted in Fig. 1) used to compute B_S .

B. Similar expressions are used to obtain (1) the percent deviation of the inverse cube field value at any one altitude from the B_L value at the same altitude starting with zero percent deviation at the earth's surface and (2) the percent deviation of the Vanguard III geomagnetic field measurement from the B_L value at the same location.

SECTION IV. PRESENTATION AND DISCUSSION OF THE RESULTS

The total geomagnetic field at 0, 100, 200, 300, 400, 600, 800, 1000, 1500, 2000, 3000, and 4000 km and at 1, 2, 4, 8, and 16 earth radii above the earth's surface was computed for the meridian planes, 80°W and 100°E , for colatitudes $0^\circ10'$, 15° , 30° , 45° , 60° , 75° , and 89° in the northern hemisphere. For these locations the field was calculated using the Jensen and Whitaker's coefficients for $S = 1$ (simple dipole), 2 (centered dipole), 3, 4, 5 (eccentric dipole), ... 296, where "S" is the total number of Legendre polynomials arranged in the Schmidt's sequence. The inverse cube field was also calculated for these locations starting with the computed earth's surface value using all the Jensen and Whitaker's coefficients (i. e., for $S = 296$).

The total field for the location, 30°N latitude and 80°W longitude (near to Cape Canaveral, Florida), from the earth's surface to 16 earth radii is shown in Figure 6 for $S = 1, 2, 3, 4, 5, 10$, and 296 and for the inverse cube relation. It can be seen that: (1) The values obtained with the inverse cube relation are larger than those using Jensen and Whitaker's coefficients and diverge with altitude, up to at least one earth radius, (2) the values at $S = 2$ and 3 are numerically closer to the values at $S = 296$ than those $S = 1, 4$, and 5, and (3) the values change relatively little from $S = 10$ to $S = 296$.

In Figs. 7 - 9 the field values are shown as a function of total number of Legendre polynomials at various altitudes above the earth's surface. It is apparent from the curves in Figs. 7 - 9 that: (1) The values fluctuate to limiting values with increasing S , (2) the magnitude of the fluctuation decreases with increasing S and altitude, and (3) for 80°W longitude the values at $S = 2$ and 3 are numerically closer to the limiting values than those for $S = 4, 5, 6$, and 7 at 60° and 89° colatitudes while at 30° colatitude this is not so. The truncation levels at 0.1, 0.5, 1, 2, and 3 percent are indicated by arrows up to 4000 km. The S value for any one percent truncation level, T , is chosen such that decreasing S by one will produce a percent value greater than that of the truncation level. Generally, the T levels shift to lower S values with increasing altitude. The S values at $T = 0.1, 0.5, 1, 2$, and 3% were computed for the altitudes and locations indicated in the first sentence of this section and plotted in the appropriate meridional cross sections at 80°W and 100°E longitudes. S isolines were then

drawn. The S-isolines for various percent truncation levels are shown in Figs. 10 and 11. From these figures it is seen that: (1) The largest S values, S gradients and S variability with latitude at any one T occur in the atmospheric surface layer, which varies from about 0 - 2000 km at $T = 0.1\%$ to about 0 - 400 km at $T = 3\%$, and (2) the S values decrease with increasing altitude.

The percent truncation levels for $S = 1, 2, 3, 4, 5, 10, 25, 50, 100, 242,$ and 279 were calculated for the altitudes and location indicated in the first sentence of this section. The largest T's, regardless of latitude, were plotted on altitude versus S cross sections for 80°W longitude and 100°E longitude; the T's at the location 30°N latitude, 80°W longitude, which is near to Cape Canaveral, Florida were also plotted on an altitude versus S cross section. T isolines were then drawn and are shown in Fig. 12. The highest T's are obtained for low altitudes and S's; the maximum value was $T = 28.1\%$, which was obtained for altitude zero and $S = 2$ in the 100°E cross section (Fig. 12b). A trough of low T's at $S = 2$ and 3 , and a ridge at $S = 4$ are present in the 80°E cross section. The isolines in Fig. 12 generally slope to lower S values with increasing altitude.

The altitude variation of T for various colatitudes at 80°W longitude is shown in Fig. 13 for $S = 1, 2, 3, 4, 5,$ and 10 and of the percent deviation for the inverse cube relation in Fig. 14. The T values below 4000 km are less for $S = 2$ and 3 , than for $S = 1, 4,$ and 5 at $45^\circ, 60^\circ, 75^\circ,$ and 89° colatitudes. The inverse cube percent deviation values generally diverge from zero at the earth's surface showing positive deviations for colatitudes $45^\circ, 60^\circ, 75^\circ,$ and 89° and on the whole below 4000 km at 80°W , the geomagnetic field values computed with the inverse cube relation are higher than the B_L values while those computed with a small number of Legendre polynomials are lower than the B_L values; the reverse situation occurs for low colatitudes.

A comparison by means of percent deviation of measured total geomagnetic fields from the B_L values computed for the measurement locations was also made. For this purpose, the 1959 Vanguard III geomagnetic field data between latitudes 2°N and 34°N and longitudes 75°W and 83°W were used. The percent deviation data were lumped into 200 km layer increments and the 5, 50, and 95 percentile levels computed. Five values, which ranged from 1.63 to 1.67% in the

3500 - 3700 km layer were excluded in computing the percentile levels since it was felt that these values were not based on representative values of the earth's main field. These percentile levels are shown in Fig. 15 along with the total range. It can be seen that from 600 to 3800 km ninety percent of the computed data lies between -1.00% and 0.30% while all the data lie between -1.00% and 0.93%. It appears, therefore, that the computed B_L values for latitudes 0 - 45°N and longitude 80°W vary from a range of 1.7 - 2.7% at 600 km to a range of 4.6 - 9.1% at 3800 km. In fact, it is not necessary to use the entire 296 Legendre polynomials to calculate B. The number to be used to give as good results should lie between those for $T = 2\%$ in Fig. 10b and those for $T = 1\%$ in Fig. 10c. The maximum number of polynomials for $T = 1\%$ and $T = 2\%$ between 600 and 3800 km from 0 - 45°N are respectively 19 and 12. Even the use of the 10 polynomials (see Figs. 12a and 13f) does not exceed $T = 2.3\%$.

By using the data in Fig. 15 as a guide line of the percent deviation of measured data from computed data bounding curves of the total geomagnetic field with altitude were computed. These bounding curves were obtained by arbitrarily adding $0.03 B_L$ to the maximum B_L value and $-0.03 B_L$ to the minimum B_L value in order to embrace expected extreme variations. The maximum and minimum B_L values for any one altitude were selected from the field values computed at intersection points over essentially a 5° latitude - 5° longitude worldwide intersection grid. In Fig. 16 are shown the curves of the minimum and maximum total earth's field with altitude, the B_L curve and the inverse cube field curve at 30°N, 80°W (near Cape Canaveral, Florida), and the bounding or envelope curves. The envelope curves from about 25,000 km to 32 earth radii were adjusted to allow for the magnetic field carried by a solar flare plasma which, in itself, can reduce or increase the geomagnetic field by approximately 100 gammas (Refs. 11 and 12).

SECTION V. CONCLUSIONS

An evaluation of the geomagnetic field equation using Jensen and Whitaker's coefficients for Epoch 1955.0 and of the inverse cube geomagnetic field equation was undertaken to 16 earth radii above the earth's surface for the regions at or near 80°W and 100°E longitudes from 0 - 90°N latitudes. From this evaluation it appears that:

1. The geomagnetic field equation using the Jensen and Whitaker's coefficients to $n = 24$, $m = 17$ (568 Gaussian coefficients, 296 Legendre polynomials) gives results much closer to the Vanguard III values ($2 - 34^\circ\text{N}$, $75 - 83^\circ\text{W}$) measured from 600 to 3800 km than does the inverse cube field equation. The deviation of $\pm 1\%$ (Fig. 15), from observed fields, of fields computed with the former equation corresponds to a maximum total of 19 Legendre polynomials necessary to compute at the truncation level of $\pm 1\%$ (Fig. 10c); the inverse cube shows a deviation of approximately 2 to 9% (Fig. 14) from the values computed by the former equation in this altitude and geographic region.

2. Reasonable envelope curves (Fig. 16) to contain the world-wide total geomagnetic field variation can be arrived at by (a) adding $+0.03 B_L$, where B_L is the value computed for $S = 296$, to the world-wide maximum B_L and $-0.03 B_L$ to the worldwide minimum B_L and (b) considering the magnetic field carried by the solar flare plasma.

3. The total field near Cape Canaveral, Florida, (Fig. 6) computed with the inverse cube relation is larger than that derived from the spherical harmonic fitted equation using Jensen and Whitaker's coefficients, and the range between them increases with altitude up to at least 1 earth radius. The values for the total number of Legendre polynomials, $S = 2$ and 3, are numerically closer to the values at $S = 296$ than those at $S = 1, 4$, and 5, and the values change relatively little from $S = 10$ to $S = 296$.

4. The total field values as a function of the total number of Legendre polynomials S (Figs. 7 - 9) (a) fluctuate to limiting values with increasing S , (b) reduce in amplitude fluctuation with increasing S and altitude, and (c) are numerically closer to $S = 296$ values for $S = 2$ and 3 than for $S = 4, 5, 6$, and 7 at 1°N , 30°N , and 80°W .

5. The largest S values, S gradients, and S variability with latitude (Figs. 10 and 11) at any one truncation level T occur in the atmospheric surface layer, which varies from about 0 - 2000 km at $T = 0.1\%$ to about 0 - 400 km at $T = 3\%$, and the S values decrease with altitude.

6. The highest percent truncation levels (T 's in Fig. 12) are obtained for low altitudes and S 's, a trough of low T 's at $S = 2$ and 3 and a ridge at $S = 4$ are present in the 80°W cross sections and absent in the 100°E cross section, and the T isolines generally slope toward lower S values with increasing altitude.

7. In general, for low latitudes below 4000 km at 80° W (Figs. 13 and 14) the geomagnetic field values computed with the inverse cube relation are higher than the $S = 296$ values while those computed for small S values are lower than the $S = 296$ values; the reverse situation holds for high latitudes.

Legendre Polynomial Number	Degree n	Order m	Legendre Polynomial Number	Degree n	Order m	Legendre Polynomial Number	Degree n	Order m
1	1	0	43	8	7	85	12	7
2	1	1	44	8	8	86	12	8
3	2	0	45	9	0	87	12	9
4	2	1	46	9	1	88	12	10
5	2	2	47	9	2	89	12	11
6	3	0	48	9	3	90	12	12
7	3	1	49	9	4			
8	3	2	50	9	5			
9	3	3	51	9	6			
10	4	0	52	9	7			
11	4	1	53	9	8			
12	4	2	54	9	9			
13	4	3	55	10	0			
14	4	4	56	10	1			
15	5	0	57	10	2			
16	5	1	58	10	3			
17	5	2	59	10	4			
18	5	3	60	10	5			
19	5	4	61	10	6			
20	5	5	62	10	7			
21	6	0	63	10	8			
22	6	1	64	10	9			
23	6	2	65	10	10			
24	6	3	66	11	0			
25	6	4	67	11	1			
26	6	5	68	11	2			
27	6	6	69	11	3			
28	7	0	70	11	4			
29	7	1	71	11	5			
30	7	2	72	11	6			
31	7	3	73	11	7			
32	7	4	74	11	8			
33	7	5	75	11	9			
34	7	6	76	11	10			
35	7	7	77	11	11			
36	8	0	78	12	0			
37	8	1	79	12	1			
38	8	2	80	12	2			
39	8	3	81	12	3			
40	8	4	82	12	4			
41	8	5	83	12	5			
42	8	6	84	12	6			

M-AERO-GS

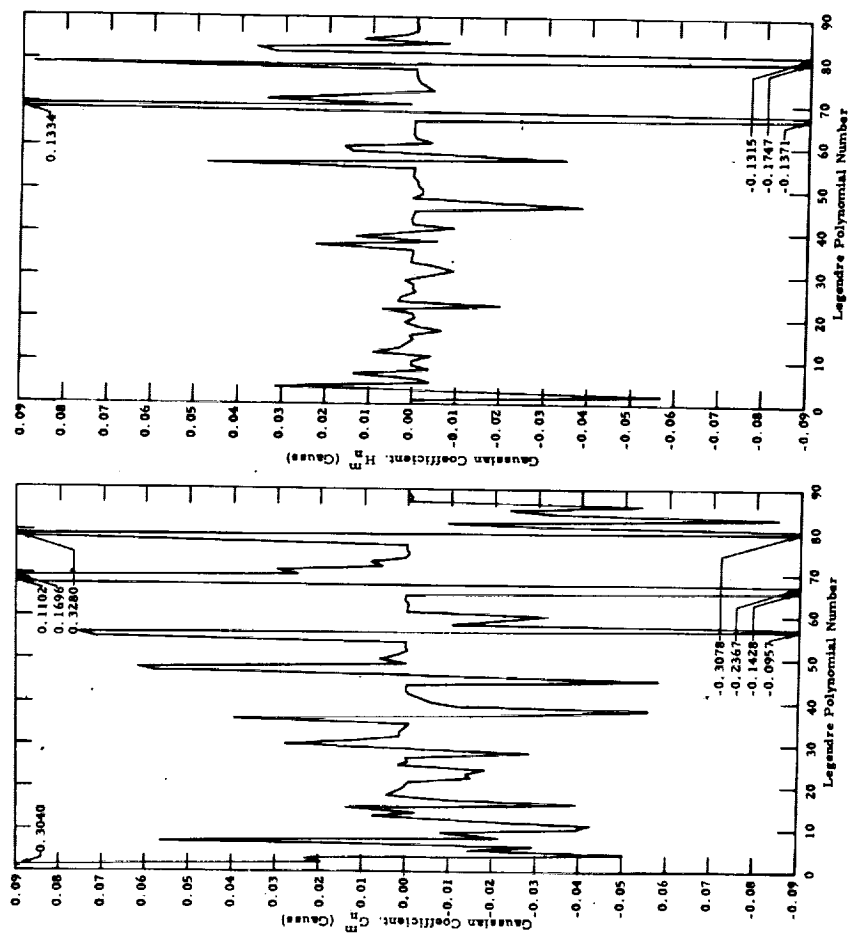
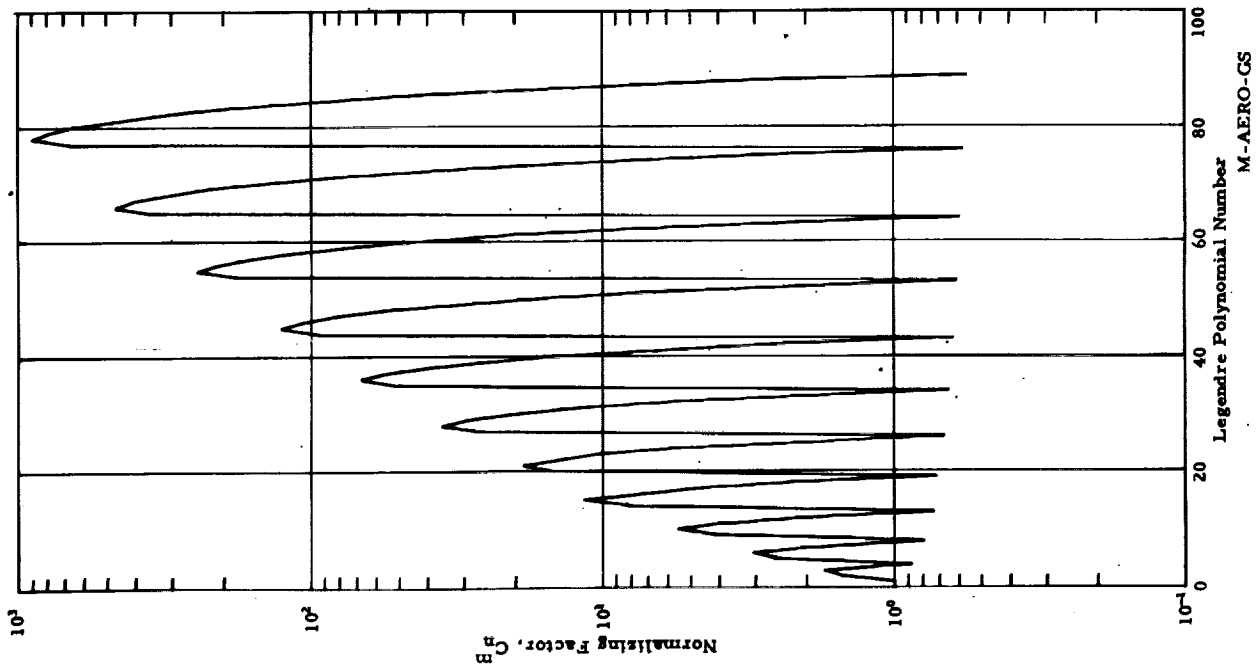


Fig. 1. Jensen and Whitaker's Normalized Gaussian Coefficients, Epoch 1955.0



Legendre Polynomial Number	Degree n	Order m	Legendre Polynomial Number	Degree n	Order m
1	1	0	43	8	7
2	1	1	44	8	8
3	2	0	45	9	0
4	2	1	46	9	1
5	2	2	47	9	2
6	3	0	48	9	3
7	3	1	49	9	4
8	3	2	50	9	5
9	3	3	51	9	6
10	4	0	52	9	7
11	4	1	53	9	8
12	4	2	54	9	9
13	4	3	55	10	0
14	4	4	56	10	1
15	5	0	57	10	2
16	5	1	58	10	3
17	5	2	59	10	4
18	5	3	60	10	5
19	5	4	61	10	6
20	5	5	62	10	7
21	6	0	63	10	8
22	6	1	64	10	9
23	6	2	65	10	10
24	6	3	66	11	0
25	6	4	67	11	1
26	6	5	68	11	2
27	6	6	69	11	3
28	7	0	70	11	4
29	7	1	71	11	5
30	7	2	72	11	6
31	7	3	73	11	7
32	7	4	74	11	8
33	7	5	75	11	9
34	7	6	76	11	10
35	7	7	77	11	11
36	8	0	78	12	0
37	8	1	79	12	1
38	8	2	80	12	2
39	8	3	81	12	3
40	8	4	82	12	4
41	8	5	83	12	5
42	8	6	84	12	6
			85	12	7
			86	12	8
			87	12	9
			88	12	10
			89	12	11
			90	12	12

Fig. 2. The Normalizing Factor, C_n^m

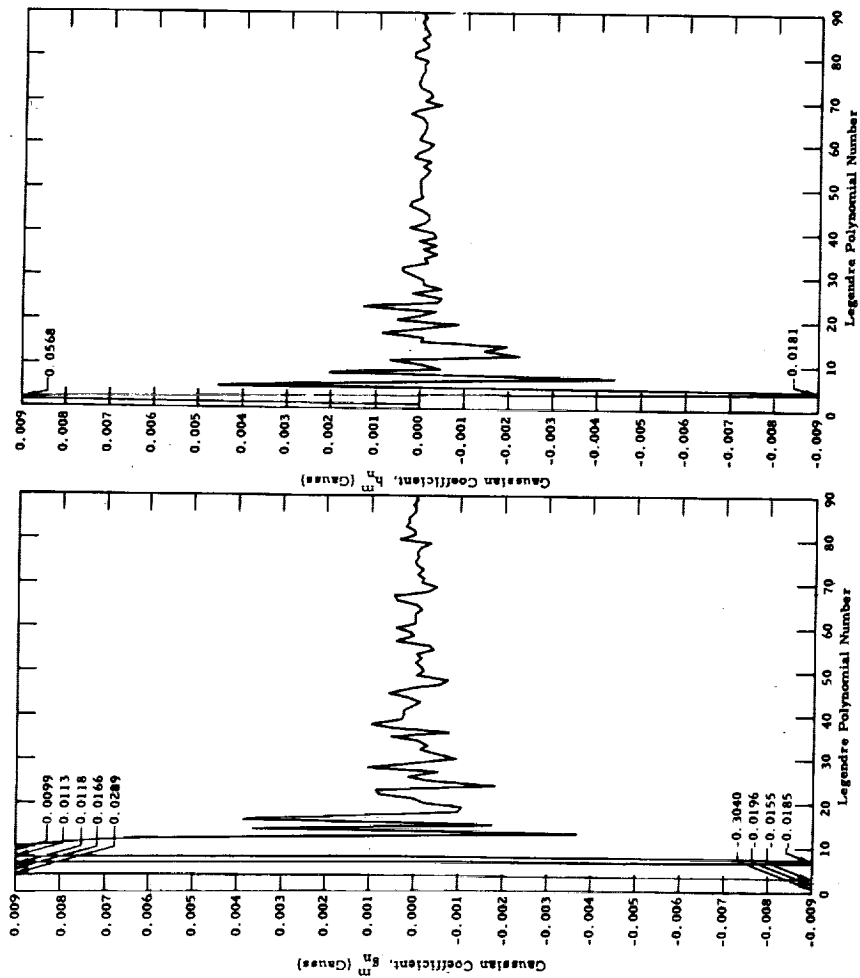


Fig. 3. Jensen and Whitaker's Unnormalized Gaussian Coefficients

Legendre Polynomial Number	Degree n	Order m	Legendre Polynomial Number	Degree n	Order m	Legendre Polynomial Number	Degree n	Order m
1	1	0	43	8	7	85	12	7
2	1	1	44	8	8	86	12	8
3	2	0	45	9	0	87	12	9
4	2	1	46	9	1	88	12	10
5	2	2	47	9	2	89	12	11
6	3	0	48	9	3	90	12	12
7	3	1	49	9	4			
8	3	2	50	9	5			
9	3	3	51	9	6			
10	4	0	52	9	7			
11	4	1	53	9	8			
12	4	2	54	9	9			
13	4	3	55	10	0			
14	4	4	56	10	1			
15	5	0	57	10	2			
16	5	1	58	10	3			
17	5	2	59	10	4			
18	5	3	60	10	5			
19	5	4	61	10	6			
20	5	5	62	10	7			
21	6	0	63	10	8			
22	6	1	64	10	9			
23	6	2	65	10	10			
24	6	3	66	11	0			
25	6	4	67	11	1			
26	6	5	68	11	2			
27	6	6	69	11	3			
28	7	0	70	11	4			
29	7	1	71	11	5			
30	7	2	72	11	6			
31	7	3	73	11	7			
32	7	4	74	11	8			
33	7	5	75	11	9			
34	7	6	76	11	10			
35	7	7	77	11	11			
36	8	0	78	12	0			
37	8	1	79	12	1			
38	8	2	80	12	2			
39	8	3	81	12	3			
40	8	4	82	12	4			
41	8	5	83	12	5			
42	8	6	84	12	6			

M-AERO-CS

Epoch	Source	Reference
1835	Gauss	5
1839	Erman-Petersen	5
1845	Adams	5
1880	Adams	5
1885	1. Fritsche 2. Schmidt 3. Neumayer-Peterson	5 5 5
1922	Dyson-Furner	5 and 7
1945	1. Afanasieva 2. Vestine-Lange 3. Fauselau-Kautzleben	5 5 8
1955	1. Finch-Leaton 2. Jensen-Whitaker	9 10

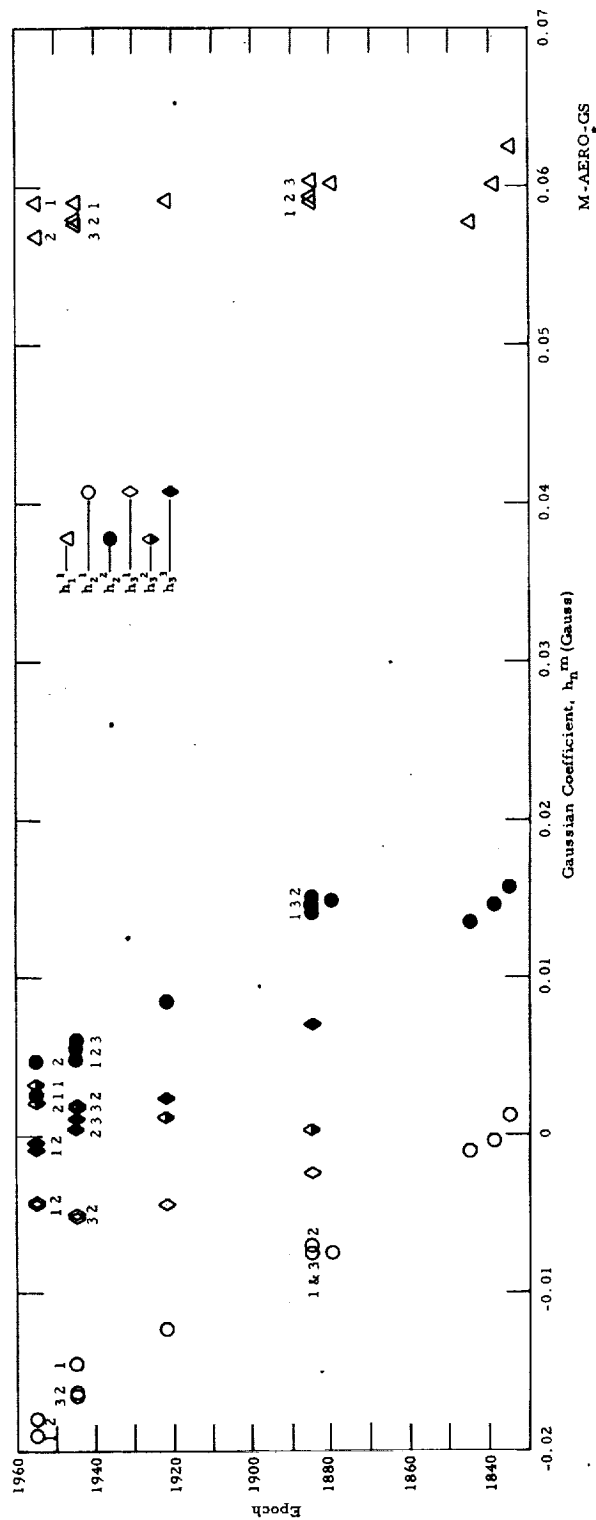


Fig. 4.b. Plot of Some Unnormalized Gaussian Coefficients h_n^m from Epochs 1835-1955

Epoch	Source	Reference
1835	Gauss	5
1839	Erman-Petersen	5
1845	Adams	5
1880	Adams	5
1885	1. Fritsche 2. Schmidt 3. Neumayer-Peterson	5 5 5
1922	Dyson-Furner	5 and 7
1945	1. Afanasieva 2. Vestine-Lange 3. Fieselau-Kautzleben	5 5 8
1955	1. Finch-Leaton 2. Jensen-Whitaker	9 10

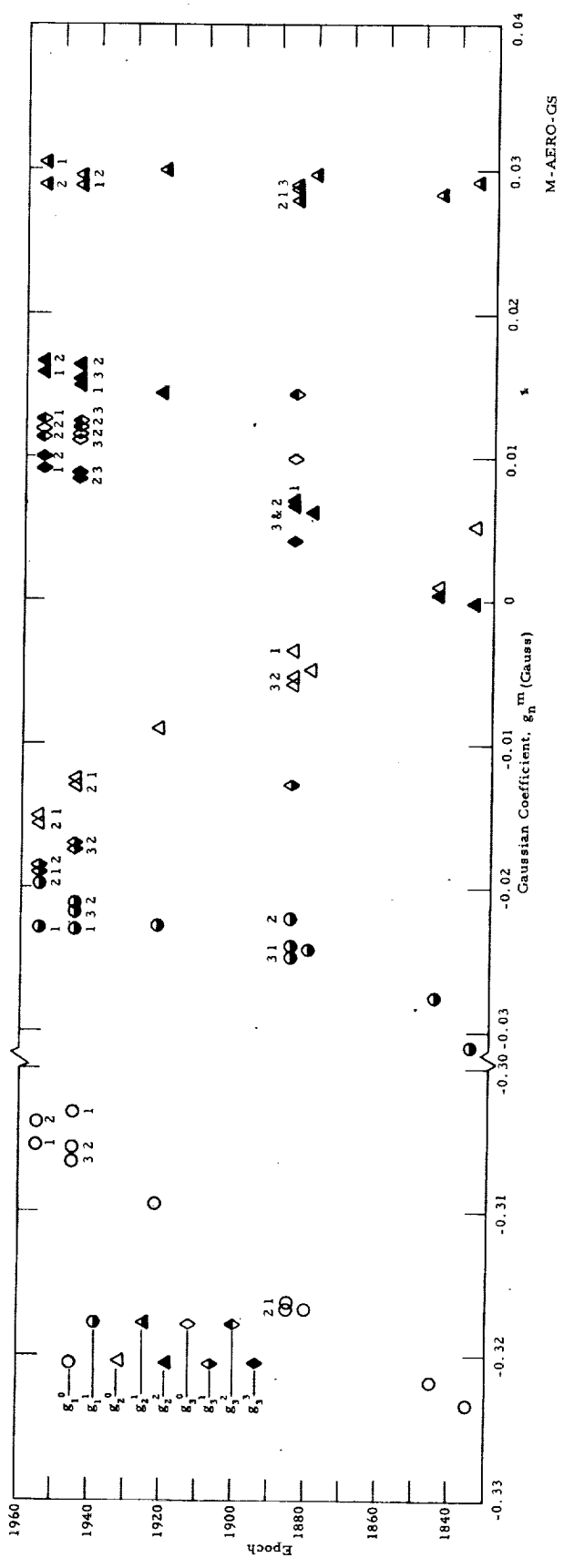


Fig. 4. a. Plot of Some Unnormalized Gaussian Coefficients g_n^m from Epochs 1835-1955

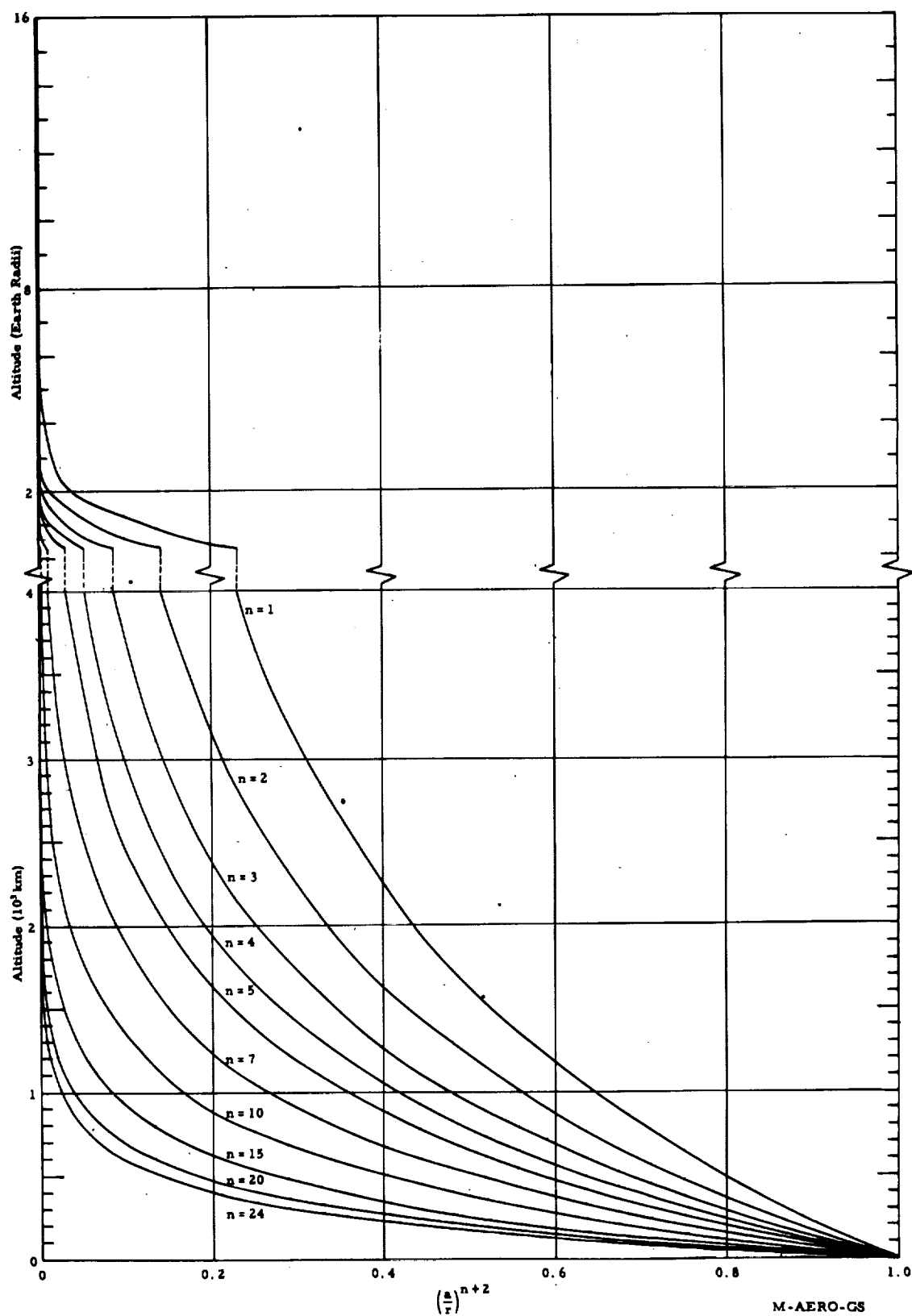


Fig. 5. Radius - Ratio Factor for Various Degrees, n

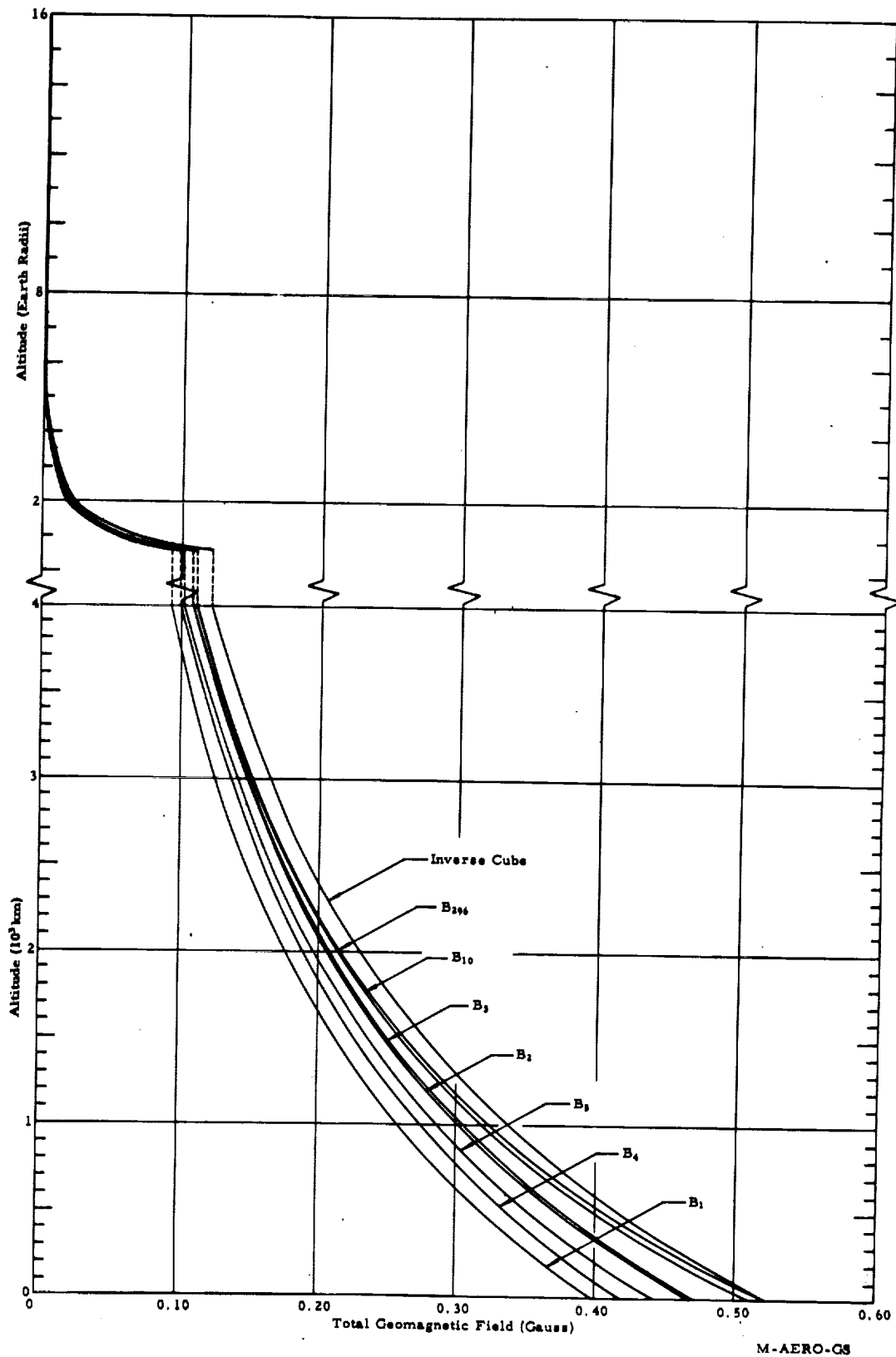


Fig. 6. Total Geomagnetic Field for Various S - Truncation Levels and for the Inverse Cube Relation for Colatitude $\theta = 60^\circ$, Longitude East $\lambda = 280^\circ$

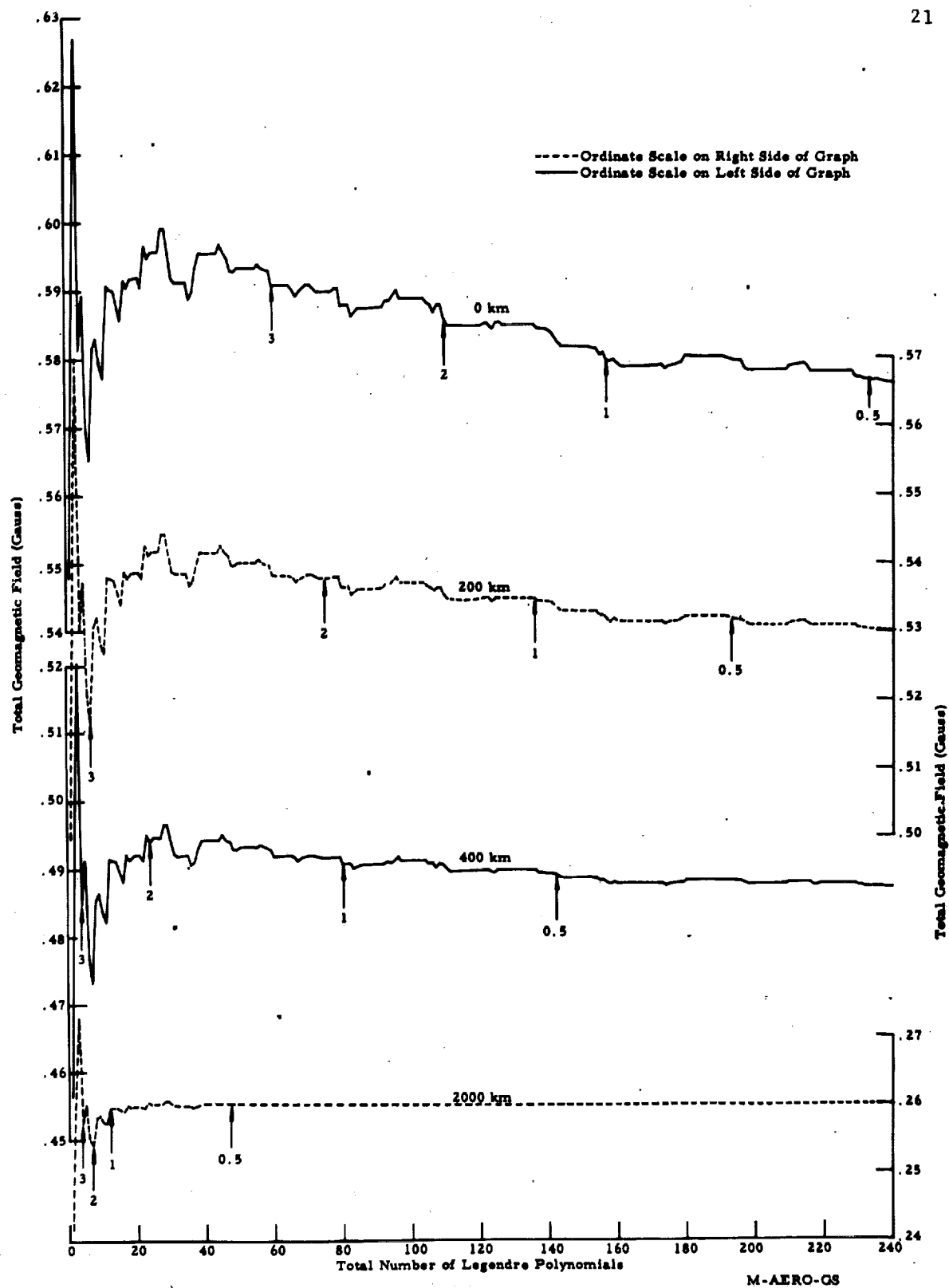


Fig. 7.a. Total geomagnetic field at various altitudes above the earth's surface for 30° colatitude, 280° E longitude. The arrows and corresponding numbers identify the percent truncation levels.

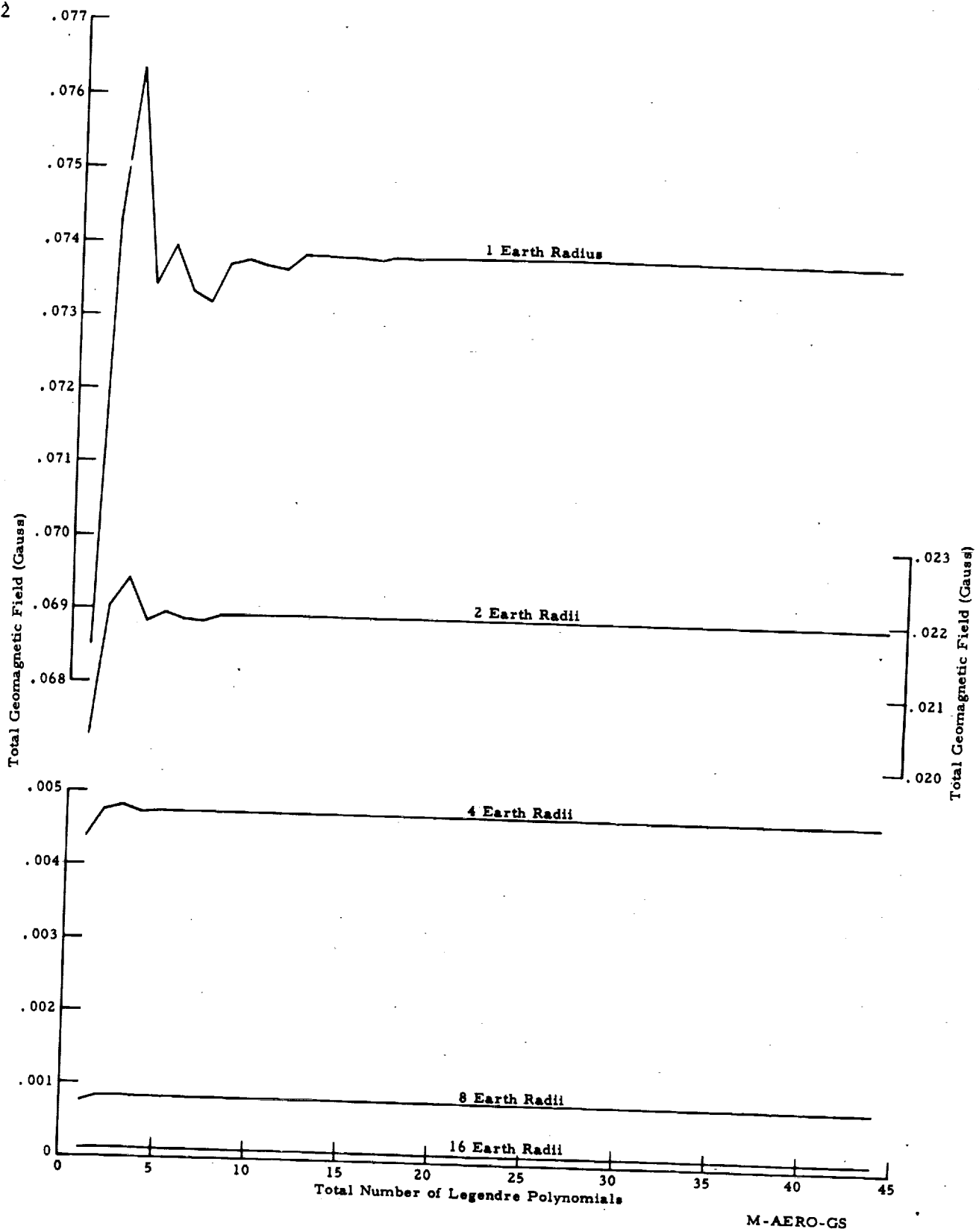


Fig. 7. b. Total geomagnetic field at various altitudes above the earth's surface for 30° colatitude, 280° E longitude

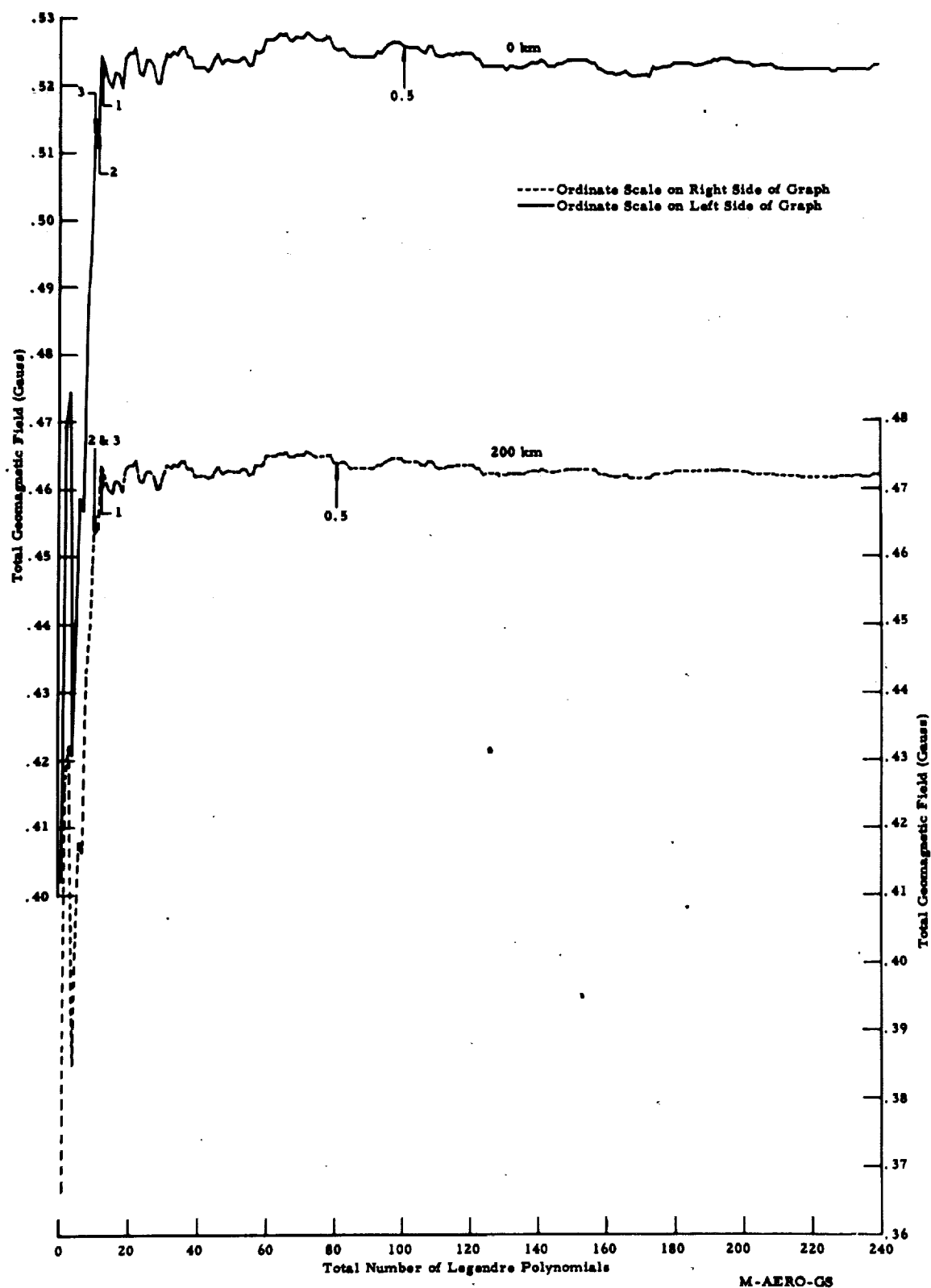


Fig. 8.a. Total geomagnetic field at various altitudes above the earth's surface for 60° colatitude, 280° E longitude. The arrows and corresponding numbers identify the percent truncation levels.

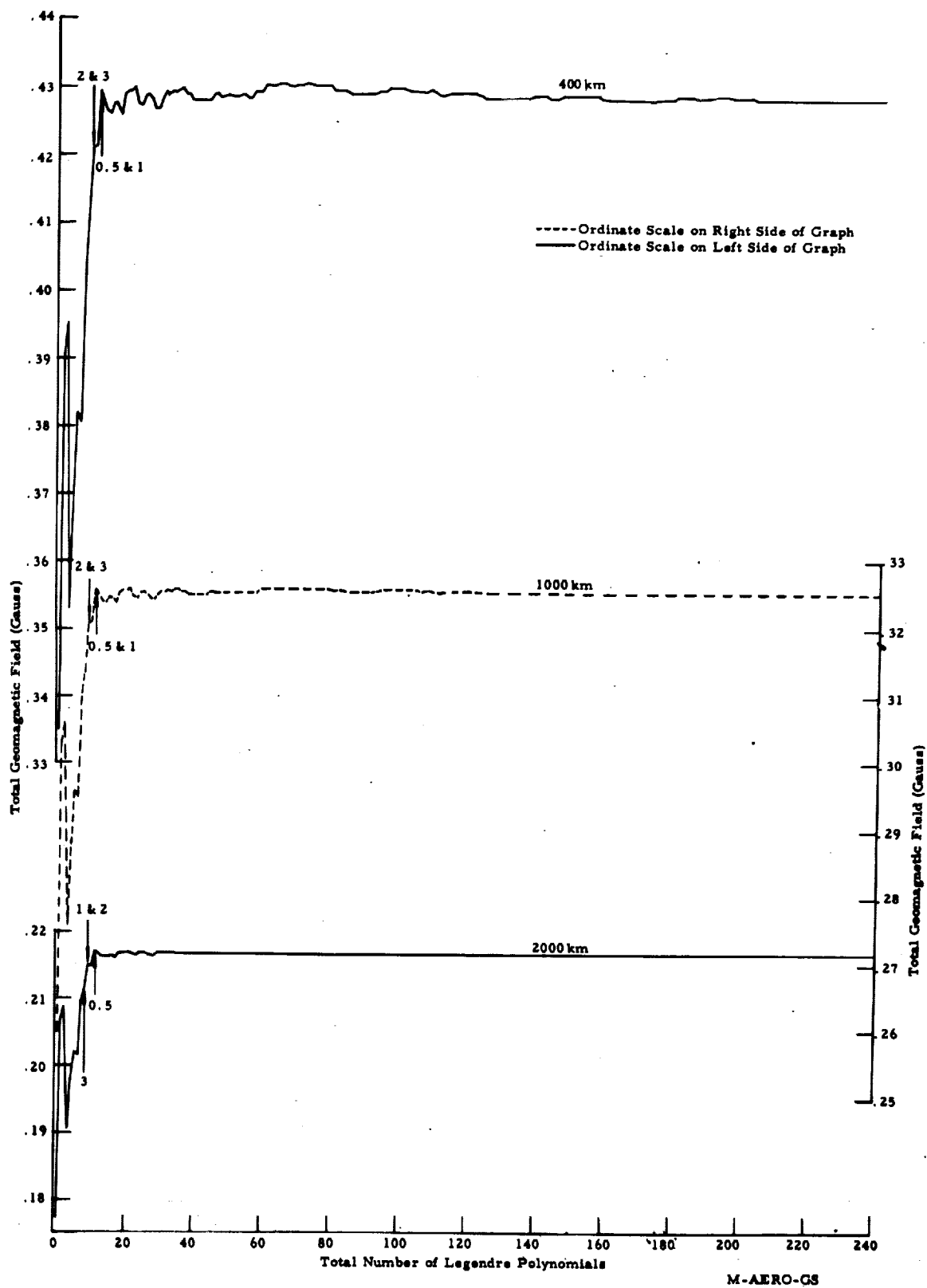


Fig. 8.5. Total geomagnetic field at various altitudes above the earth's surface for 60° colatitude, 280° E longitude. The arrows and corresponding numbers identify the percent truncation levels

M-AERO-GS

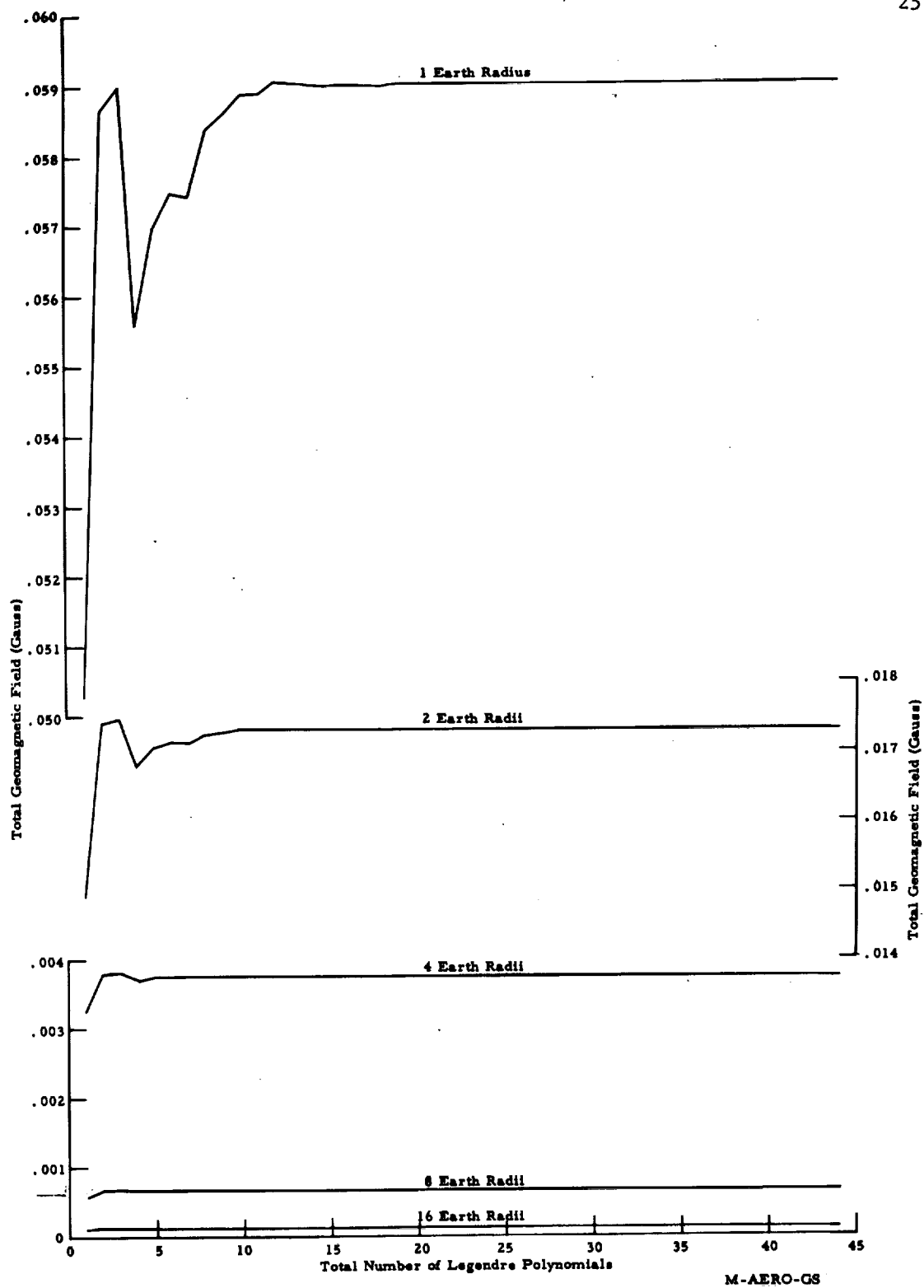


Fig. 8. e. Total geomagnetic field at various altitudes above the earth's surface for 60° colatitude, 280° E longitude.

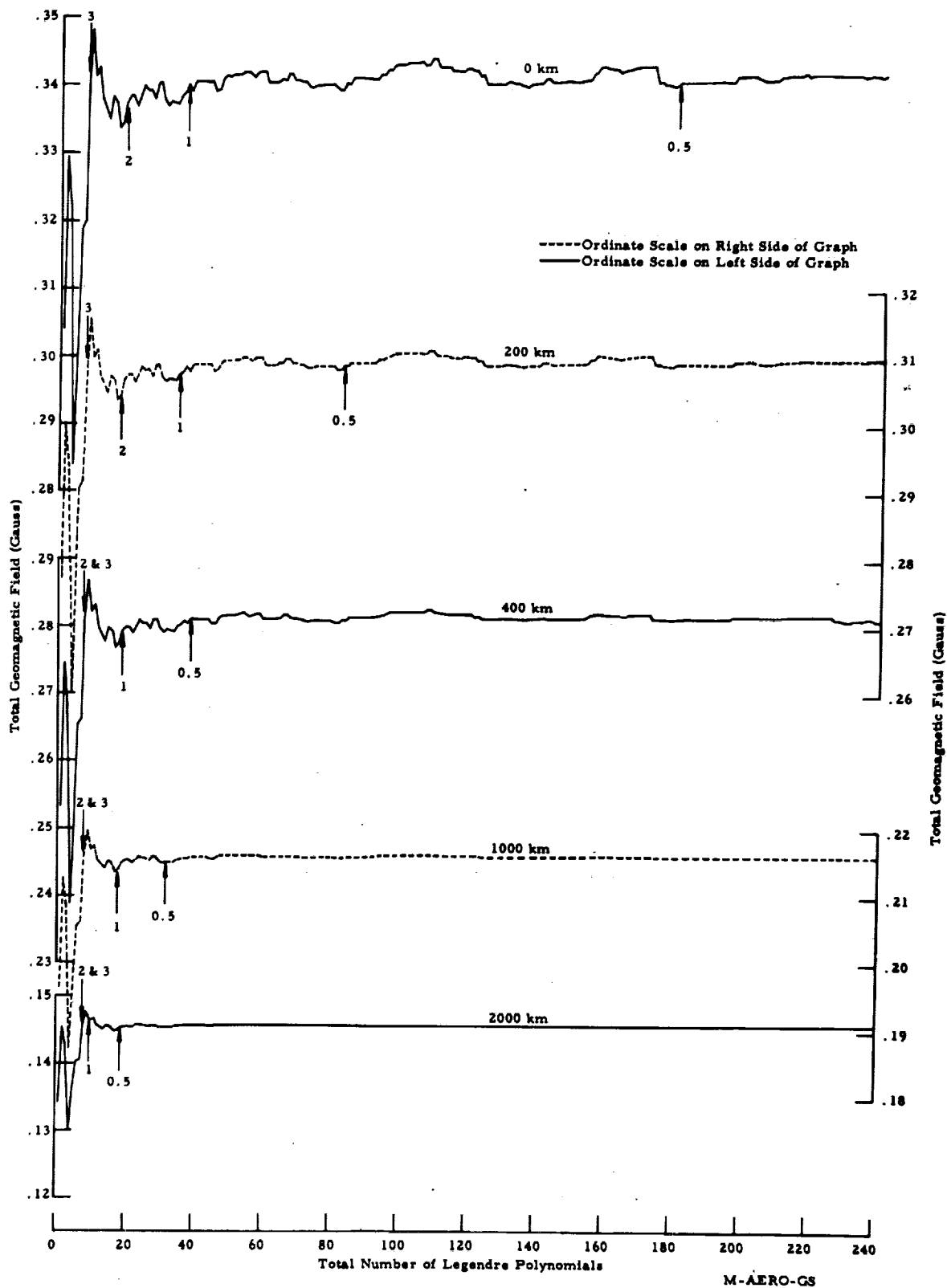


Fig. 9a. Total geomagnetic field at various altitudes above the earth's surface for 89° colatitude, 280° E longitude. The arrows and corresponding numbers identify the percent truncation levels.

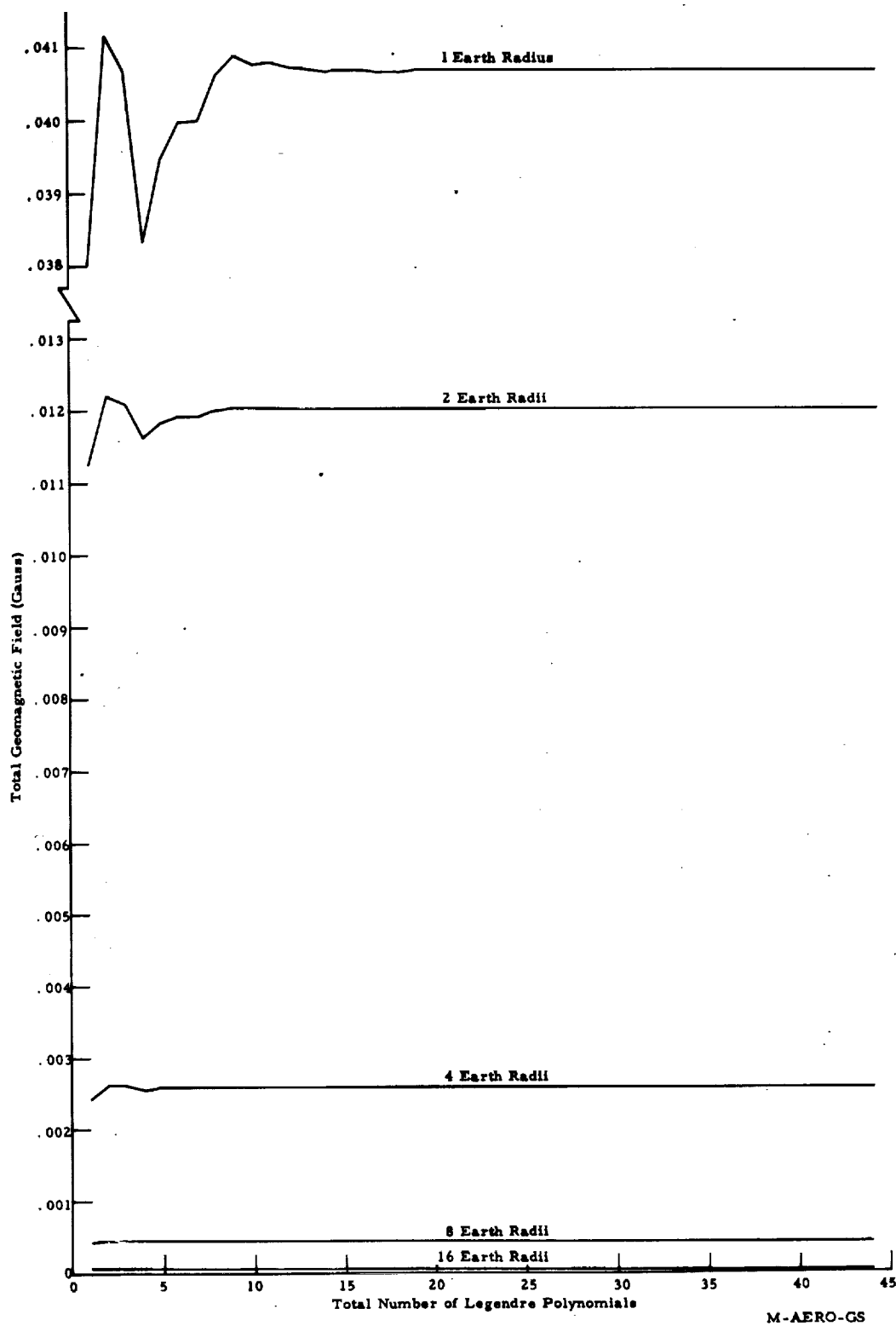


Fig. 9. b. Total geomagnetic field at various altitudes above the earth's surface for 89° colatitude, 280° E longitude.

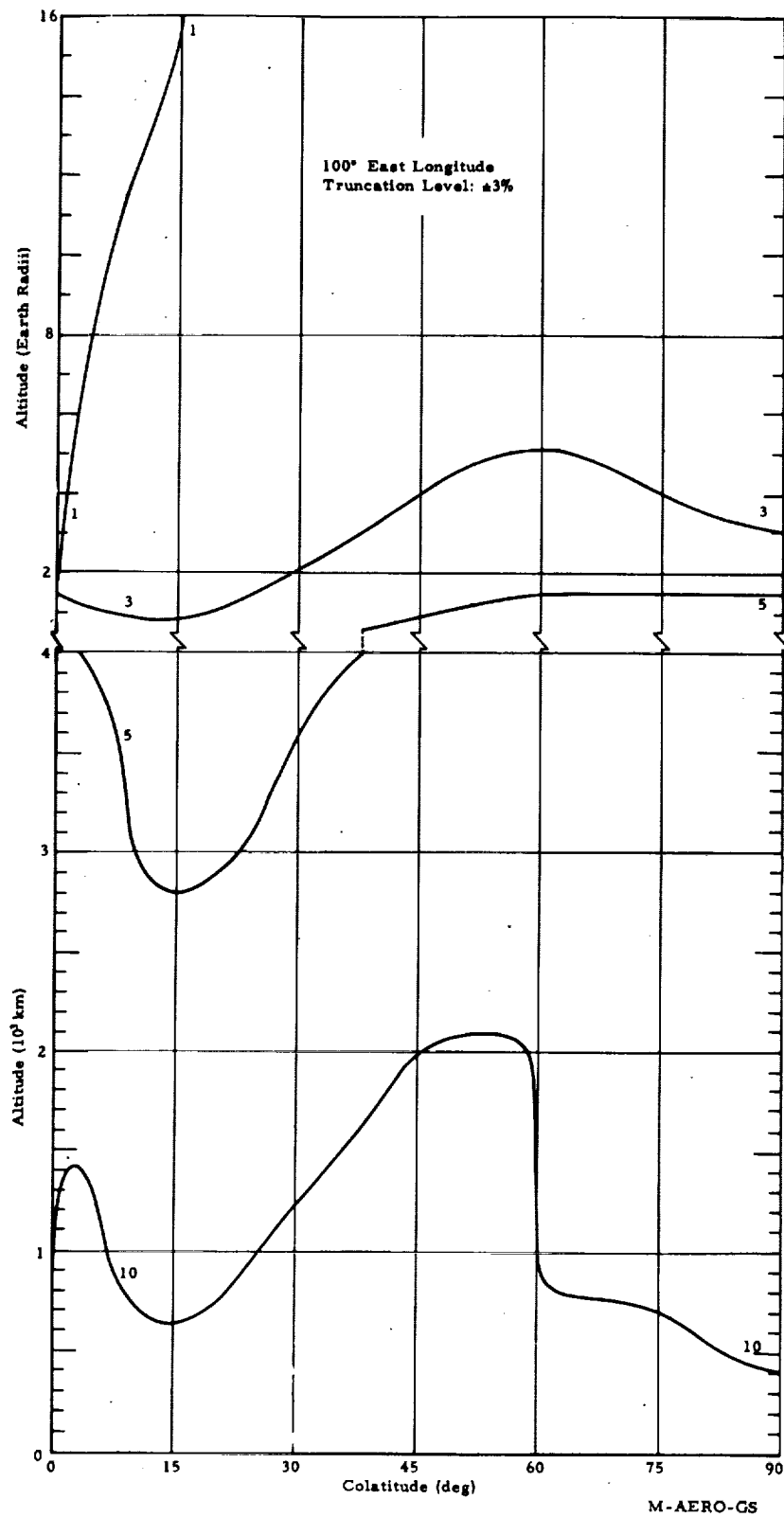


Fig. 10.a. Cross section of the number of Legendre polynomials necessary to attain the truncation level of $\pm 3\%$ difference from the total geomagnetic field value computed with 296 Legendre polynomials. Jensen and Whitaker's 568 Gaussian coefficients ($1 \leq n \leq 24$; $0 \leq m \leq 17$) for Epoch 1955.0 were used. The isolines are labeled in units of number of Legendre polynomials, S .

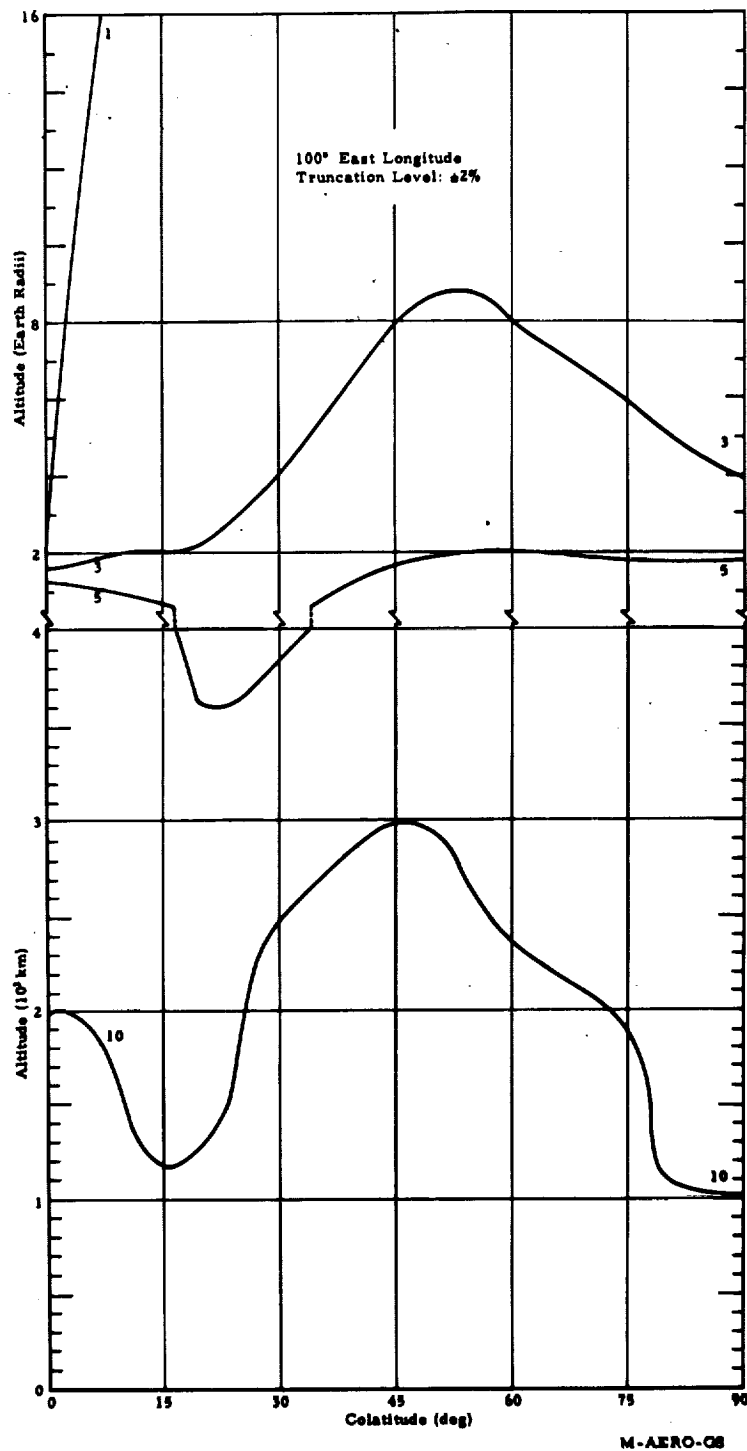


Fig. 10.b. Cross section of the number of Legendre polynomials necessary to attain the truncation level of $\pm 2\%$ difference from the total geomagnetic field value computed with 296 Legendre polynomials. Jensen and Whitaker's 568 Gaussian coefficients ($1 \leq n \leq 24$; $0 \leq m \leq 17$) for Epoch 1955.0 were used. The isolines are labeled in units of number of Legendre polynomials, S .

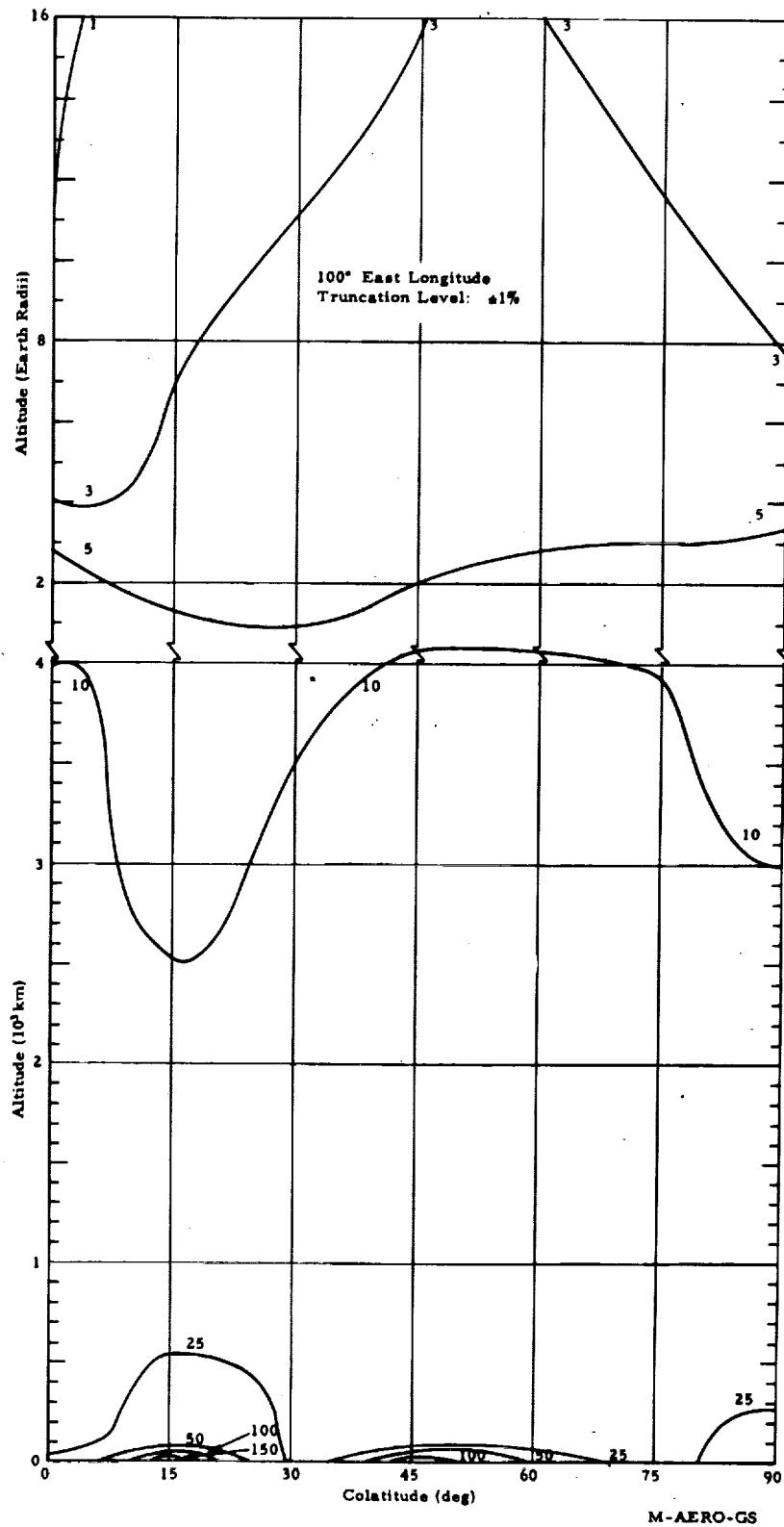


Fig 10. c. Cross section of the number of Legendre polynomials necessary to attain the truncation level of $\pm 1\%$ difference from the total geomagnetic field value computed with 296 Legendre polynomials. Jensen and Whitaker's 568 Gaussian coefficients ($1 \leq n \leq 24$; $0 \leq m \leq 17$) for Epoch 1955.0 were used. The isolines are labeled in units of number of Legendre polynomials, S .

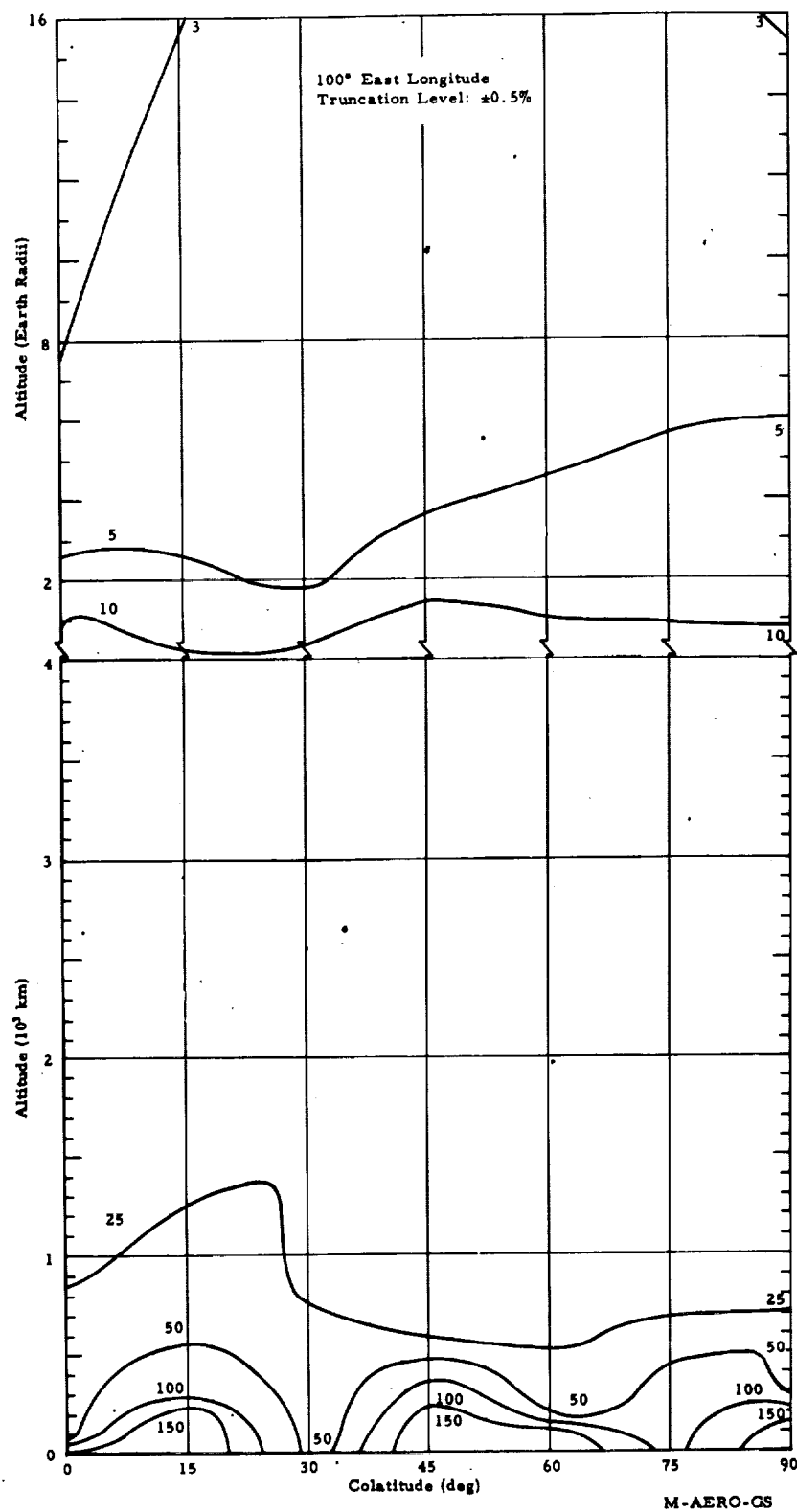


Fig. 10.d. Cross section of the number of Legendre polynomials necessary to attain the truncation level of $\pm 0.5\%$ difference from the total geomagnetic field value computed with 296 Legendre polynomials. Jensen and Whitaker's 568 Gaussian coefficients ($1 \leq n \leq 24$; $0 \leq m \leq 17$) for Epoch 1955.0 were used. The isolines are labeled in units of number of Legendre polynomials, S .

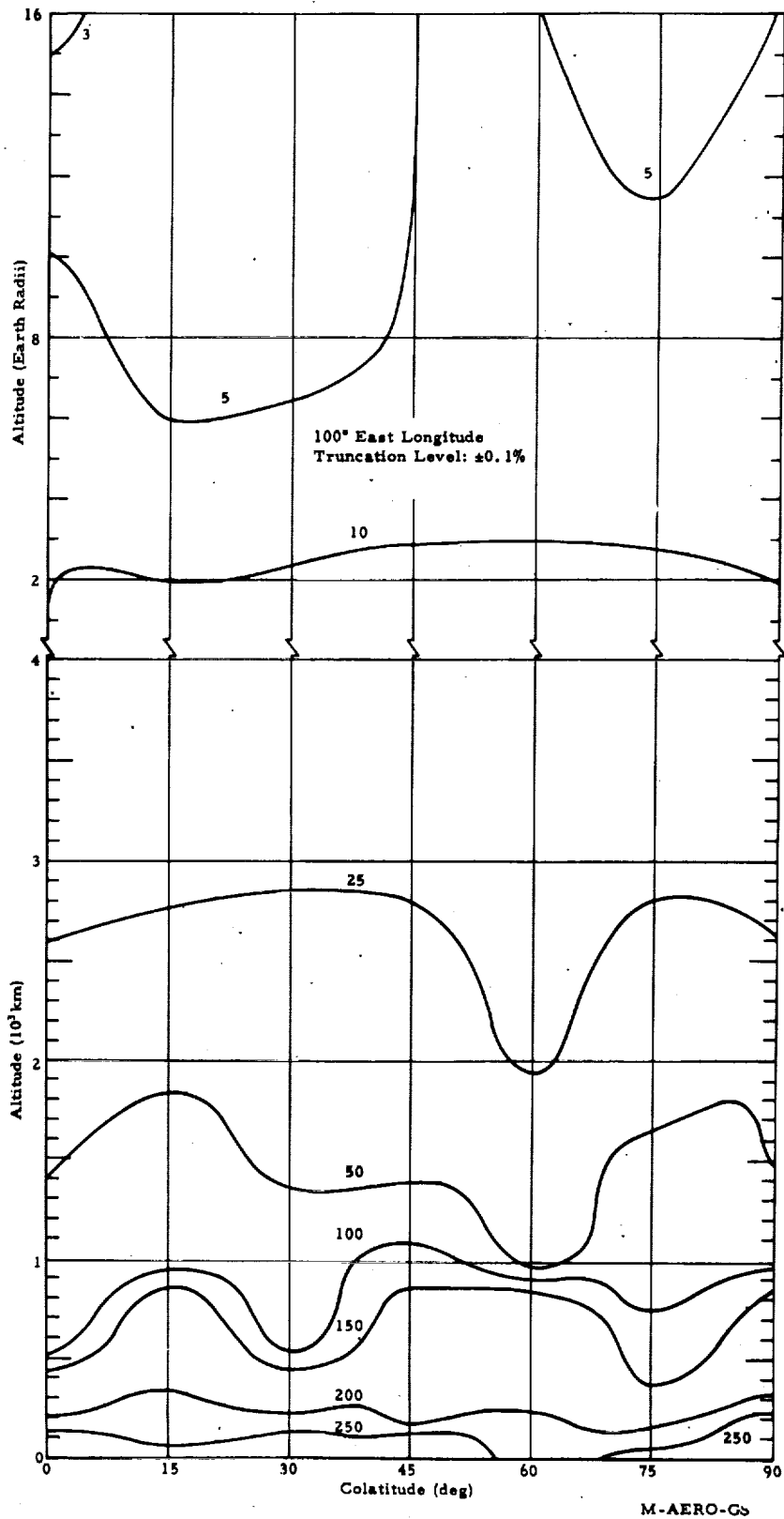


Fig. 10. e. Cross section of the number of Legendre polynomials necessary to attain the truncation level of $\pm 0.1\%$ difference from the total geomagnetic field value computed with 296 Legendre polynomials. Jensen and Whitaker's 568 Gaussian coefficients ($1 \leq n \leq 24$; $0 \leq m \leq 17$) for Epoch 1955.0 were used. The isolines are labeled in units of number of Legendre polynomials, S .

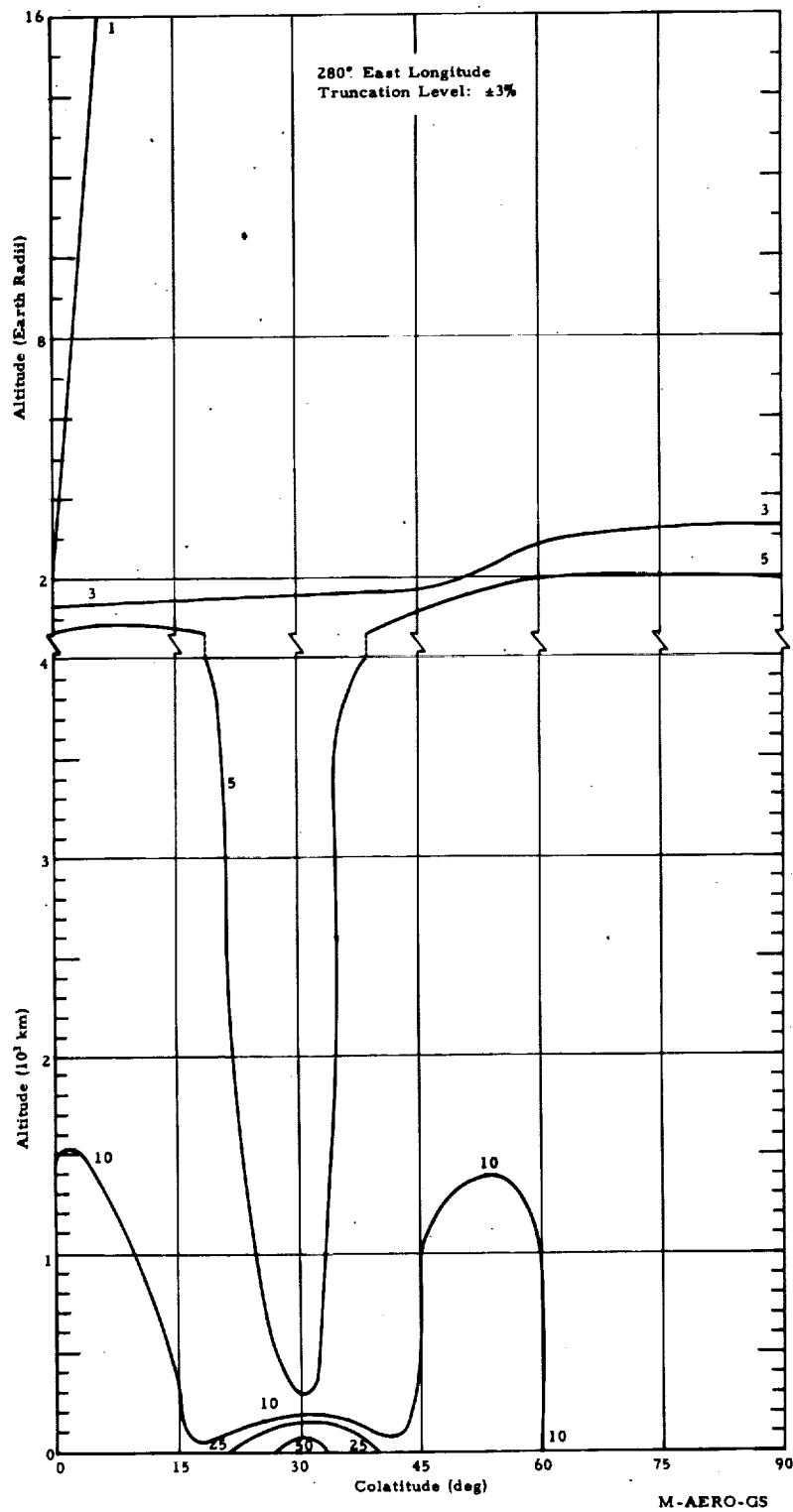


Fig. 11.a. Cross section of the number of Legendre polynomials necessary to attain the truncation level of $\pm 3\%$ difference from the total geomagnetic field value computed with 296 Legendre polynomials. Jensen and Whitaker's 568 Gaussian coefficients ($1 \leq n \leq 24$; $0 \leq m \leq 17$) for Epoch 1955.0 were used. The isolines are labeled in units of number of Legendre polynomials, S .

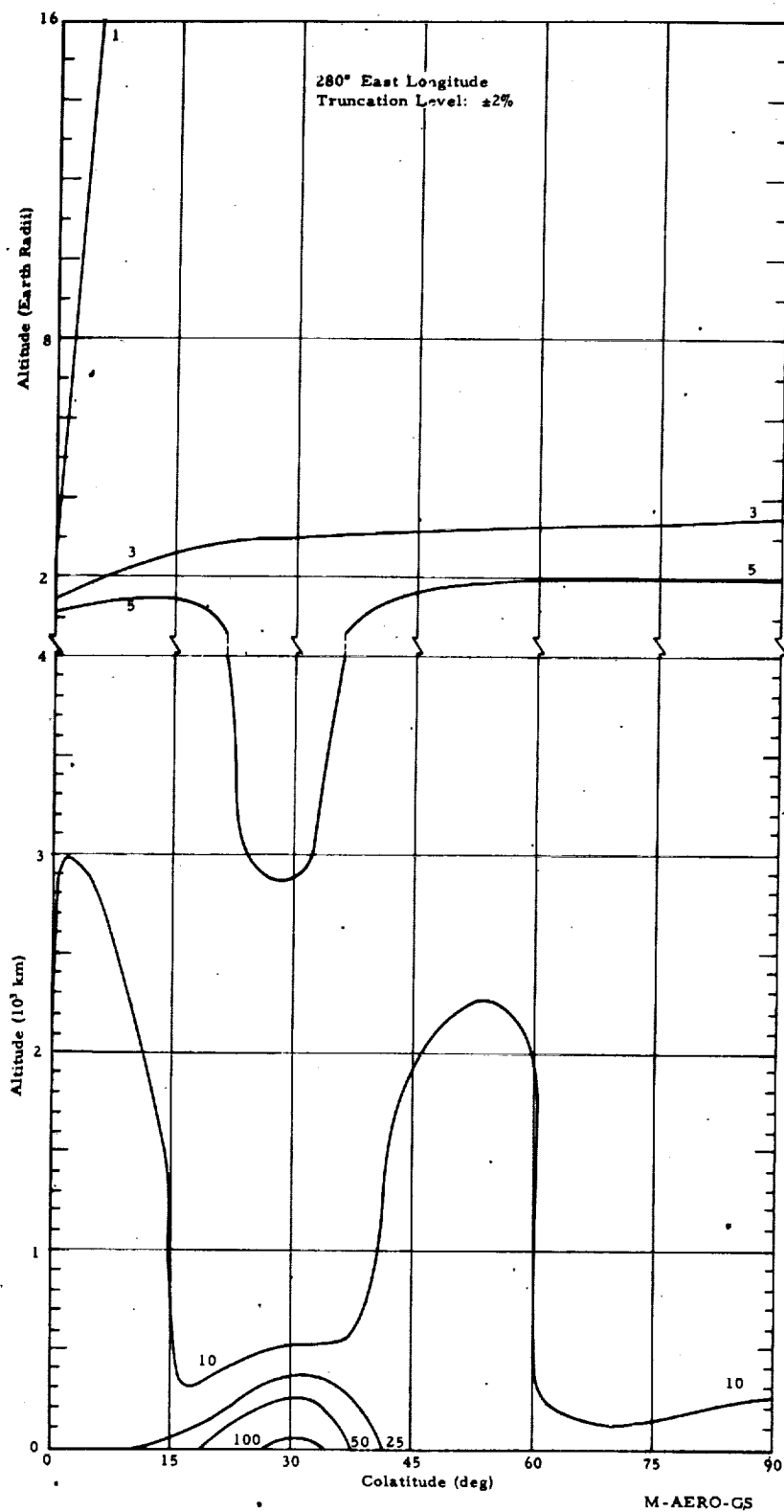


Fig. 11. b. Cross section of the number of Legendre polynomials necessary to attain the truncation level of $\pm 2\%$ difference from the total geomagnetic field value computed with 296 Legendre polynomials. Jensen and Whitaker's 568 Gaussian coefficients ($1 \leq n \leq 24$; $0 \leq m \leq 17$) for Epoch 1955.0 were used. The isolines are labeled in units of number of Legendre polynomials, S .

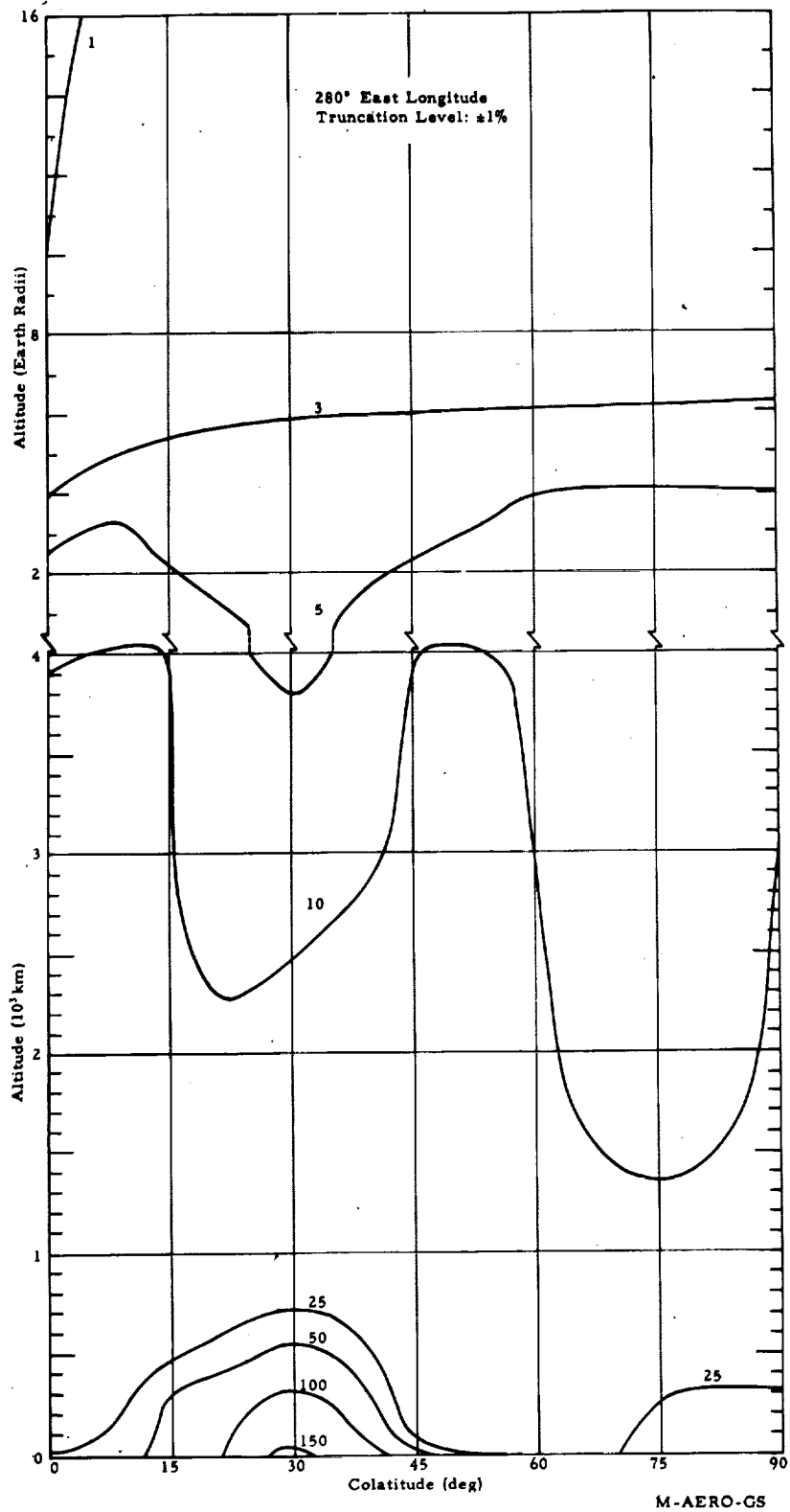


Fig. 11.c. Cross section of the number of Legendre polynomials necessary to attain the truncation level of $\pm 1\%$ difference from the total geomagnetic field value computed with 296 Legendre polynomials. Jensen and Whitaker's 568 Gaussian coefficients ($1 \leq n \leq 24$; $0 \leq m \leq 17$) for Epoch 1955.0 were used. The isolines are labeled in units of number of Legendre polynomials, S .

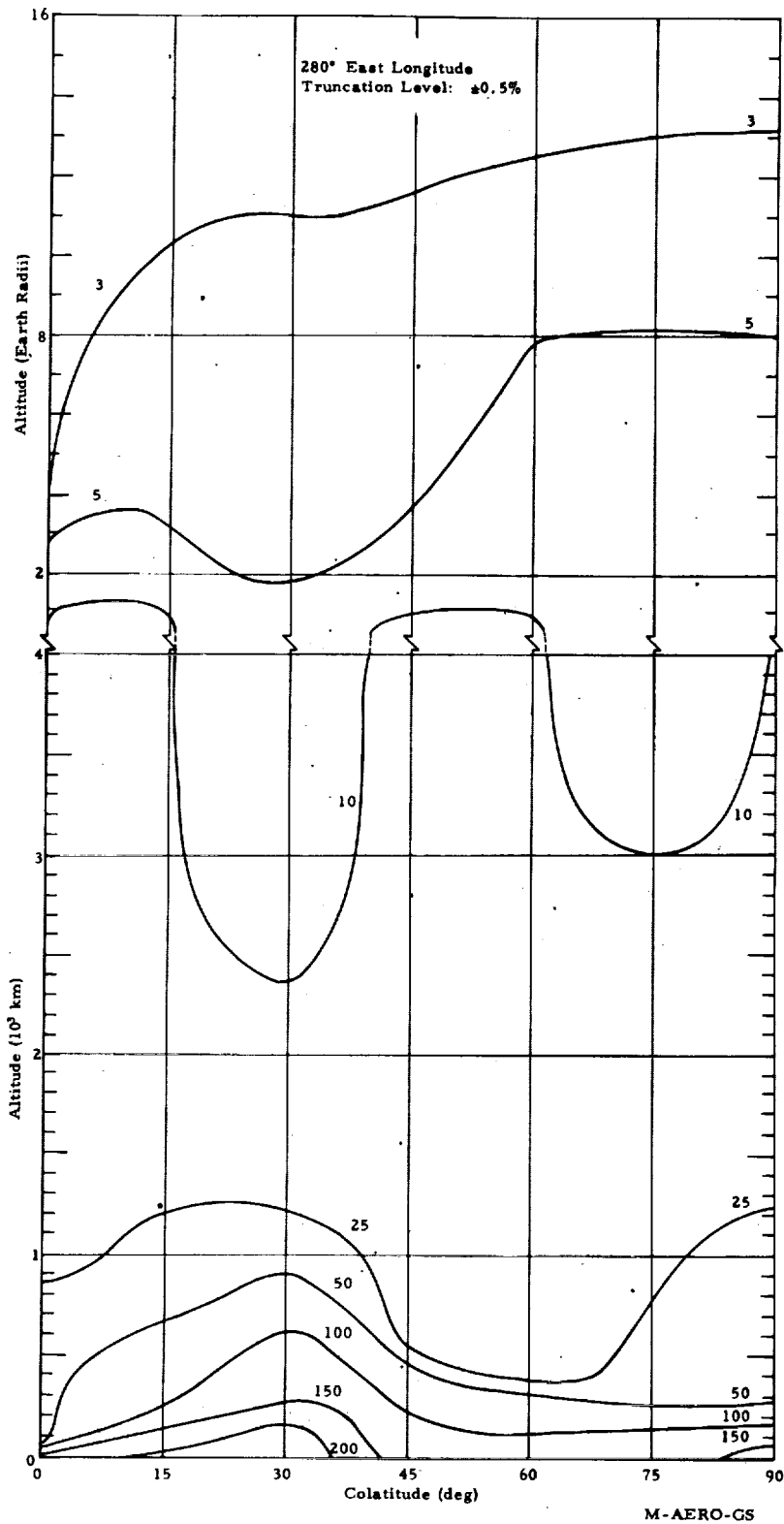


Fig. 11.d. Cross section of the number of Legendre polynomials necessary to attain the truncation level of $\pm 0.5\%$ difference from the total geomagnetic field value computed with 296 Legendre polynomials. Jensen and Whitaker's 568 Gaussian coefficients ($1 \leq n \leq 24$; $0 \leq m \leq 17$) for Epoch 1955.0 were used. The isolines are labeled in units of number of Legendre polynomials, S .

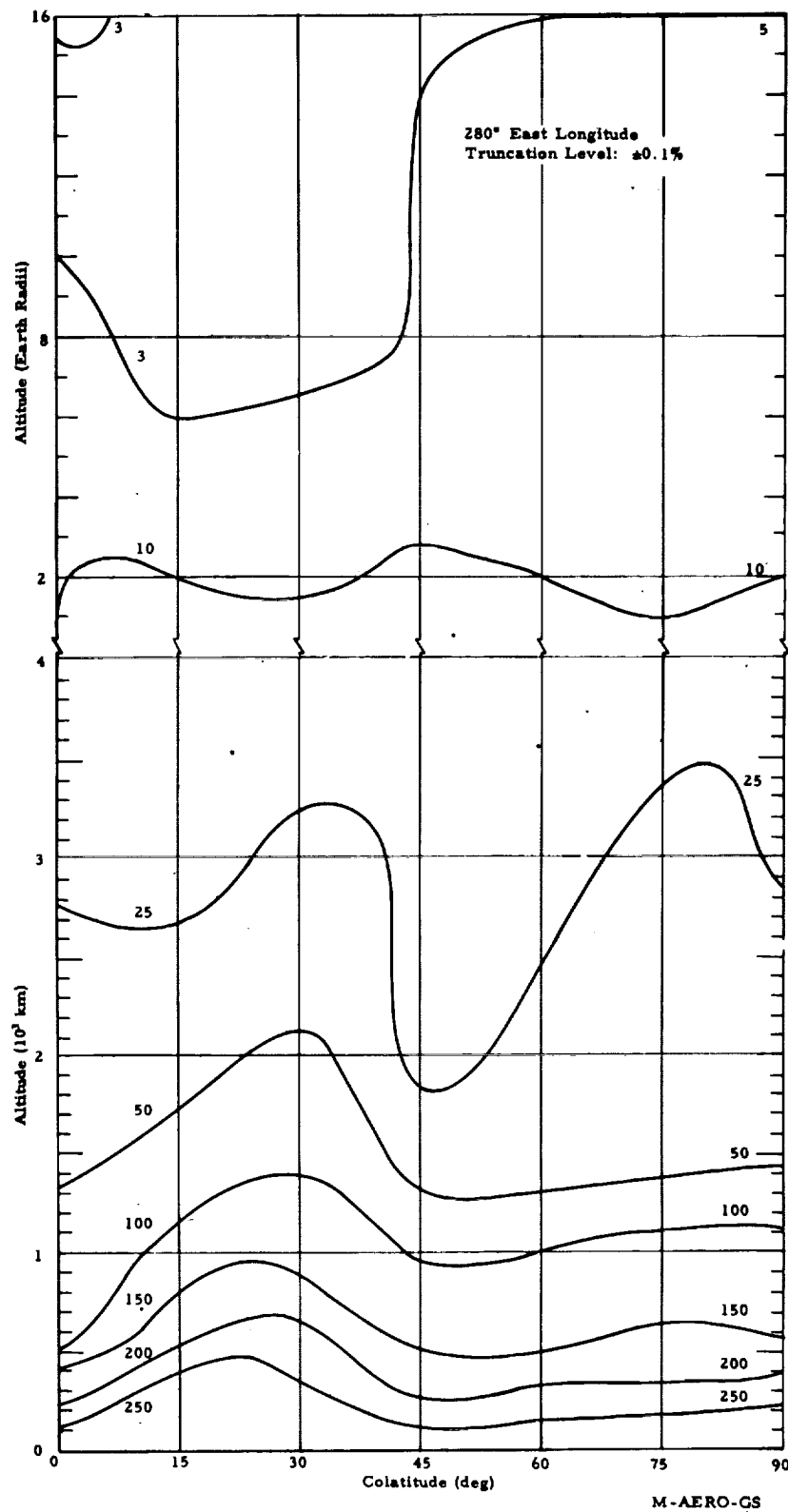


Fig. 11. e. Cross section of the number of Legendre polynomials necessary to attain the truncation level of $\pm 0.1\%$ difference from the total geomagnetic field value computed with 296 Legendre polynomials. Jensen and Whitaker's 568 Gaussian coefficients ($1 \leq n \leq 24$; $0 \leq m \leq 17$) for Epoch 1955.0 were used. The isolines are labeled in units of number of Legendre polynomials, S.

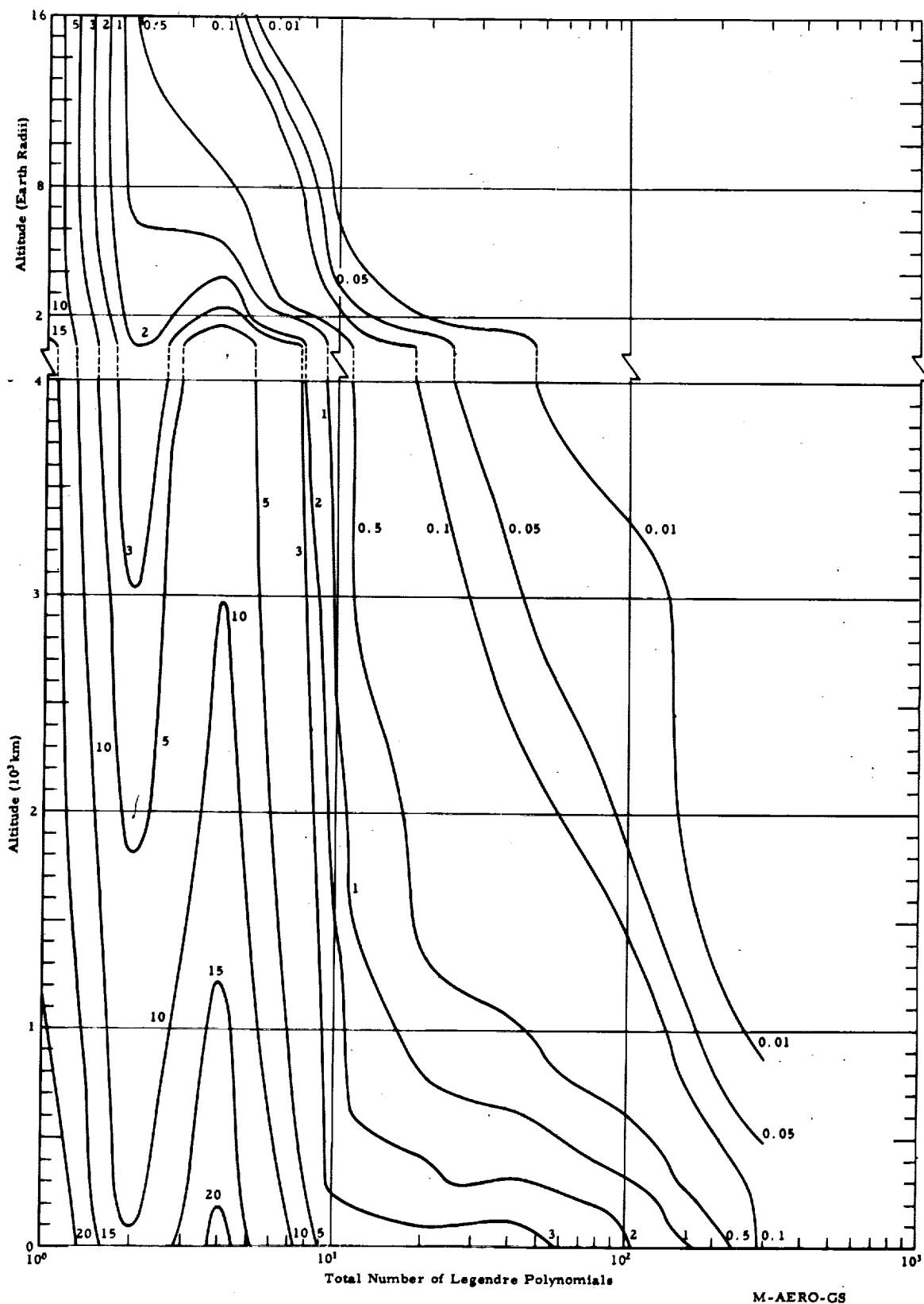


Fig. 12.a. Cross section of the maximum percent truncation levels for 280° E longitude. The isolines are in percent units.

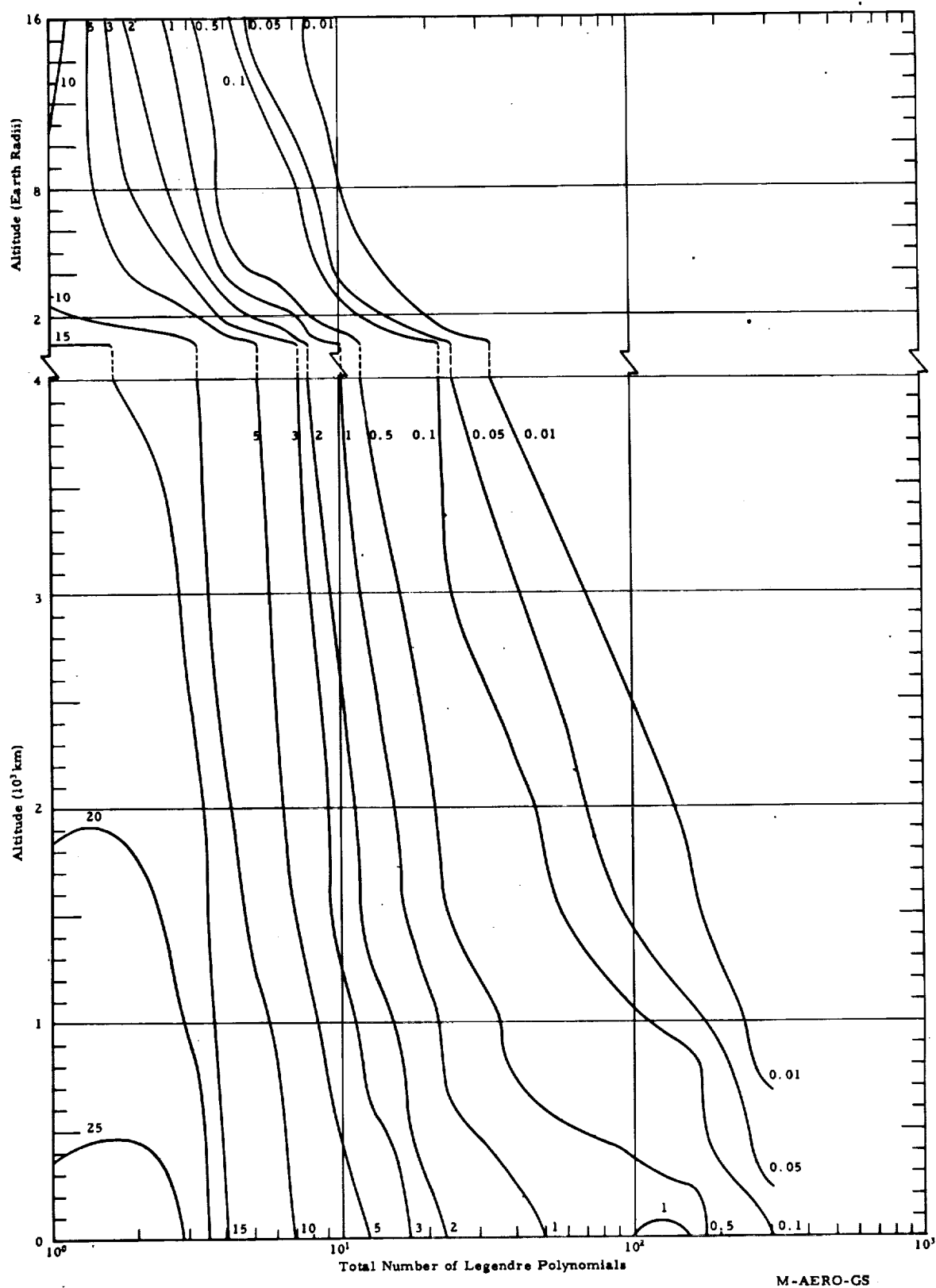


Fig. 12.b. Cross section of the maximum percent truncation levels for 100° E longitude. The isolines are in percent units.

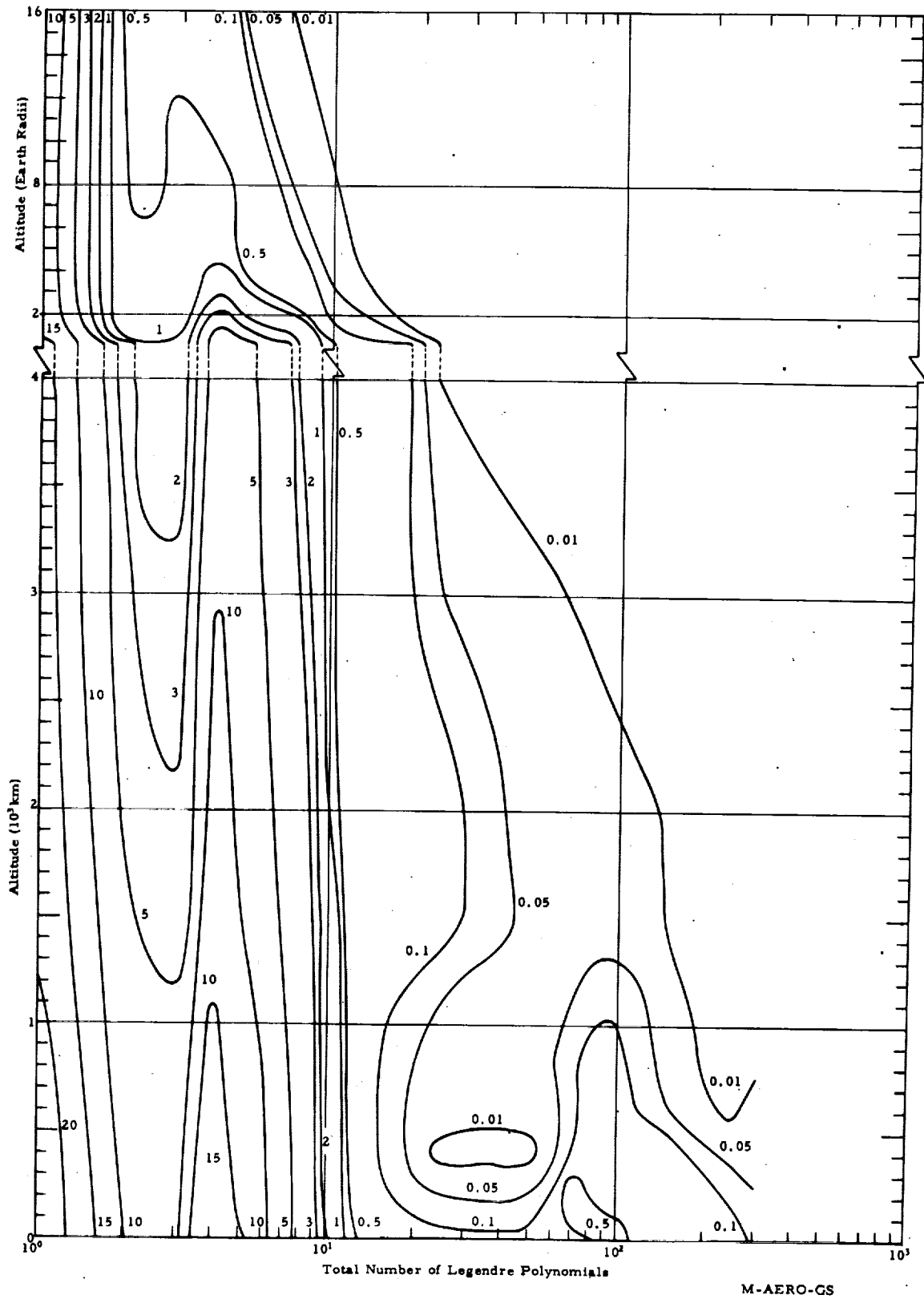


Fig. 12.c. Cross section of the percent truncation levels at 60° colatitude, 280° E longitude. The isolines are in percent units.

M-AERO-GS

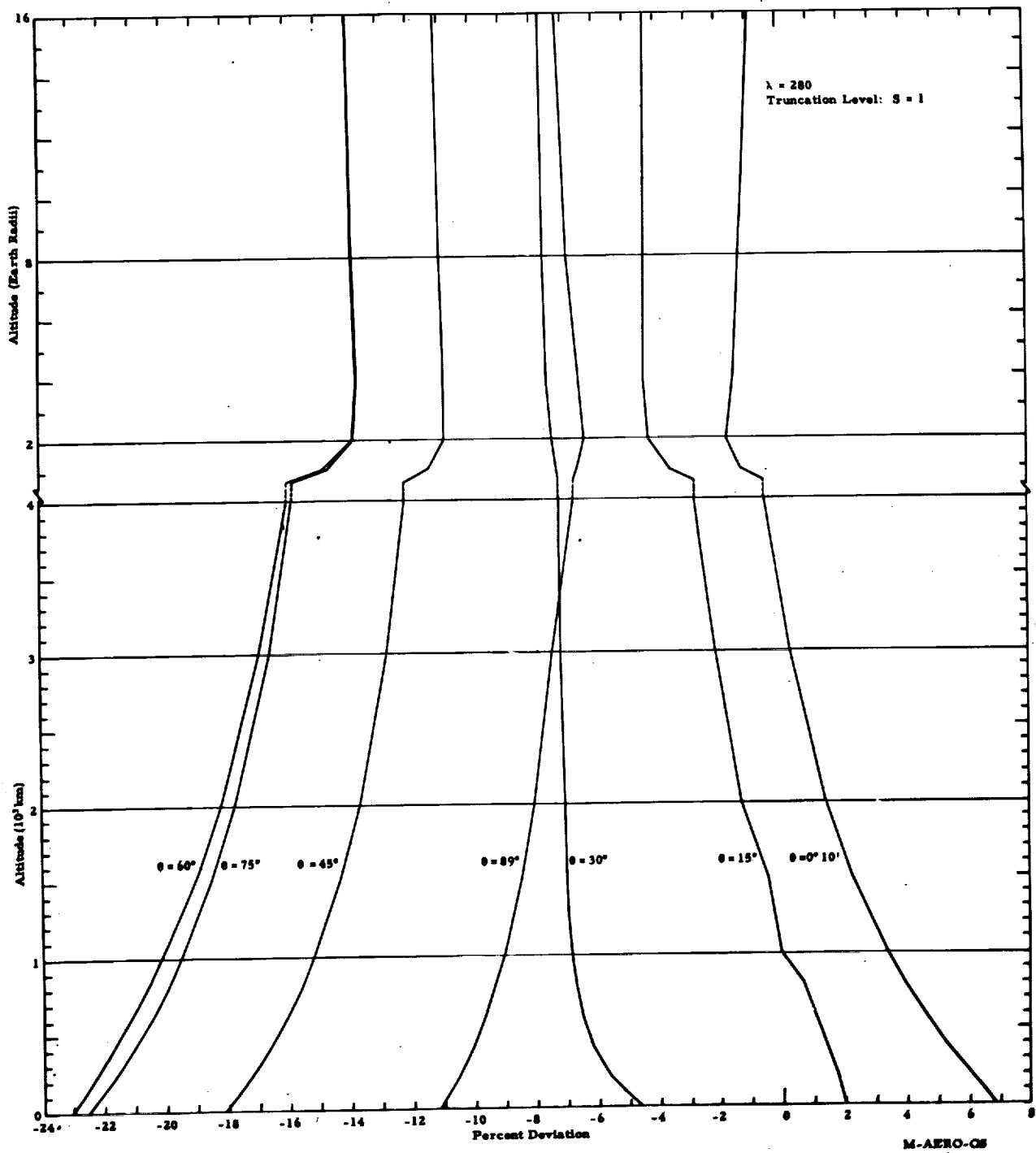


Fig. 13.a. Percent Truncation Levels at Various Colatitudes for $S = 1$

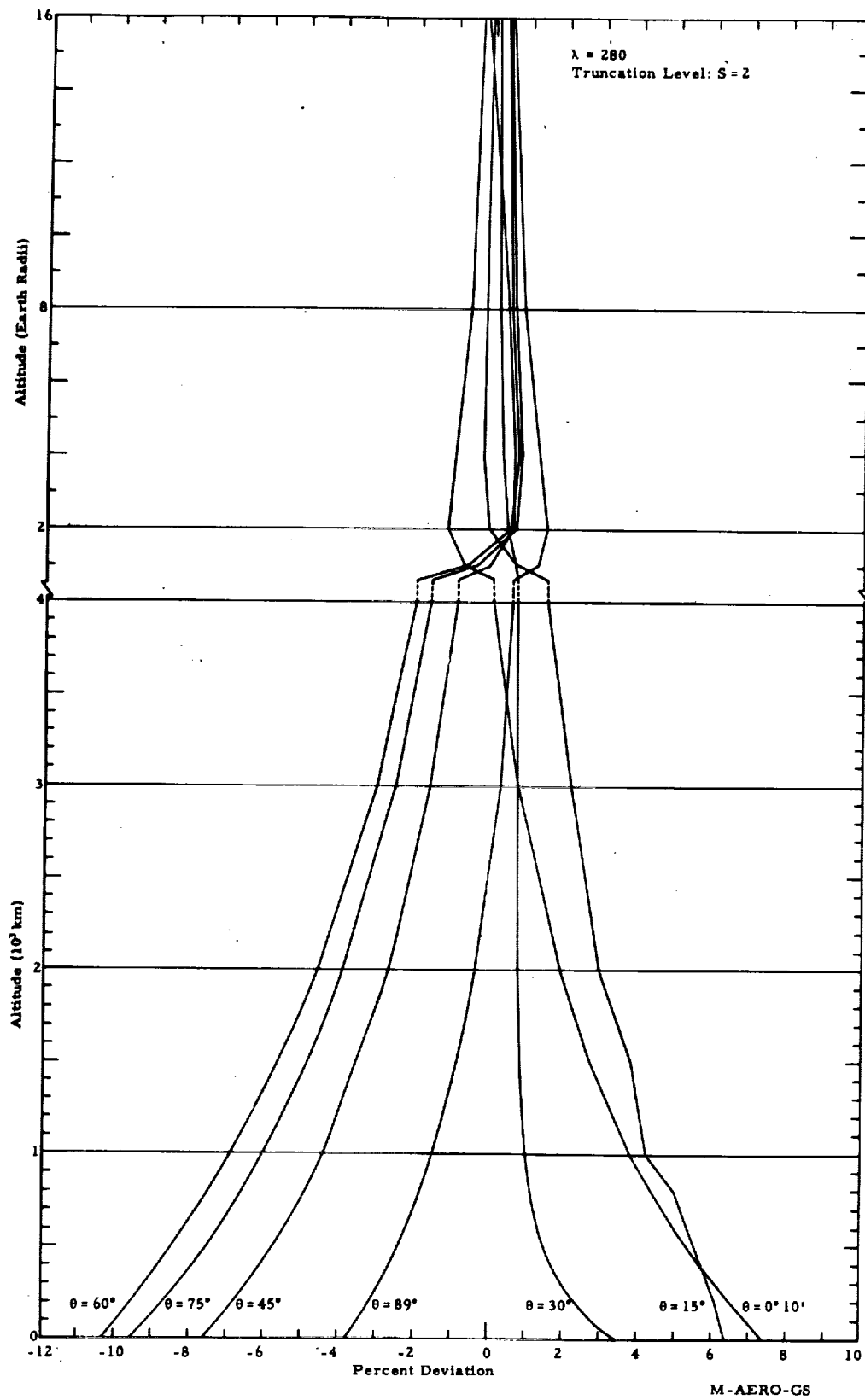


Fig. 13. b. Percent Truncation Levels at Various Colatitudes for $S = 2$

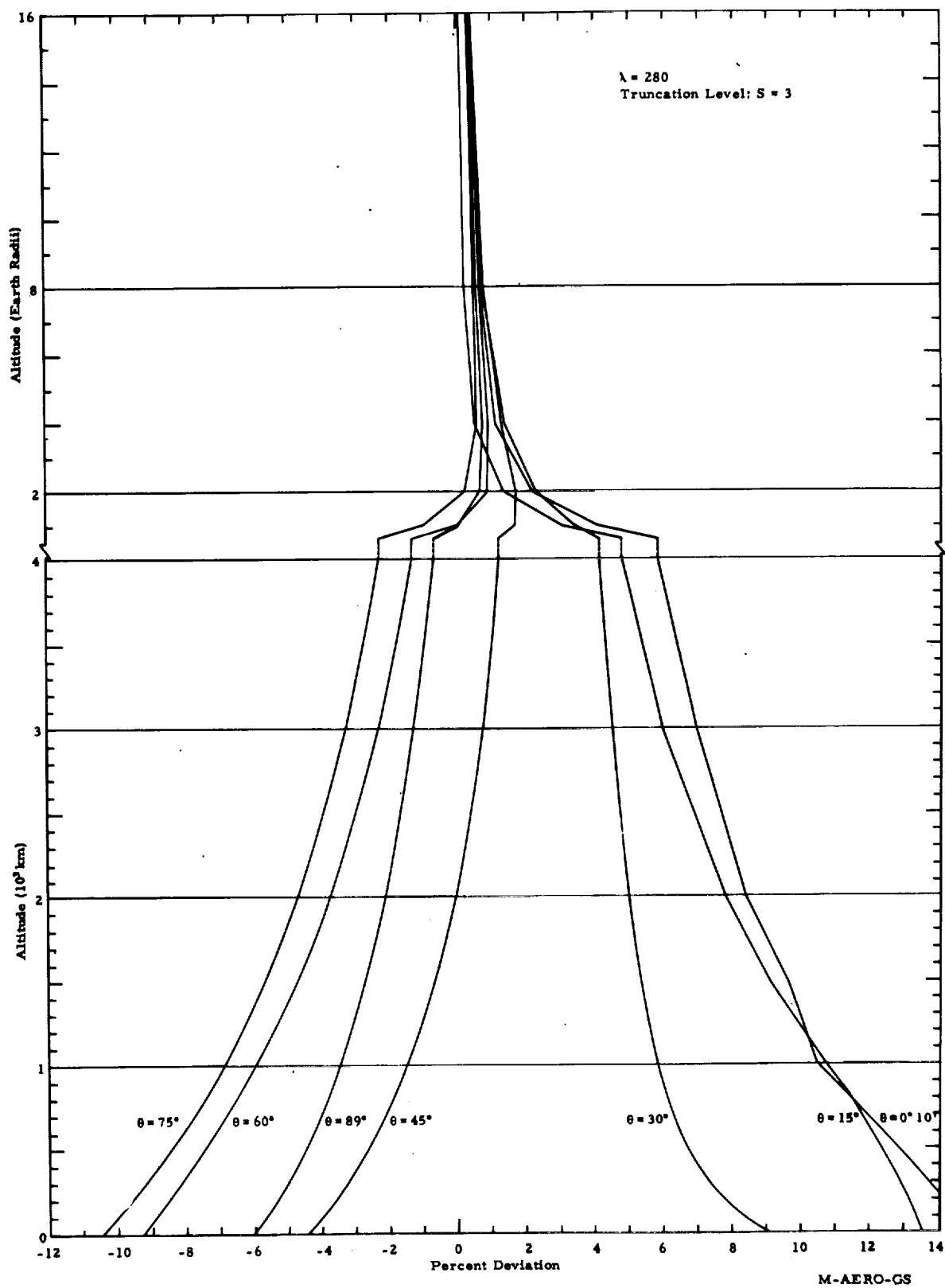


Fig. 13.c. Percent Truncation Levels at Various Colatitudes for $S = 3$

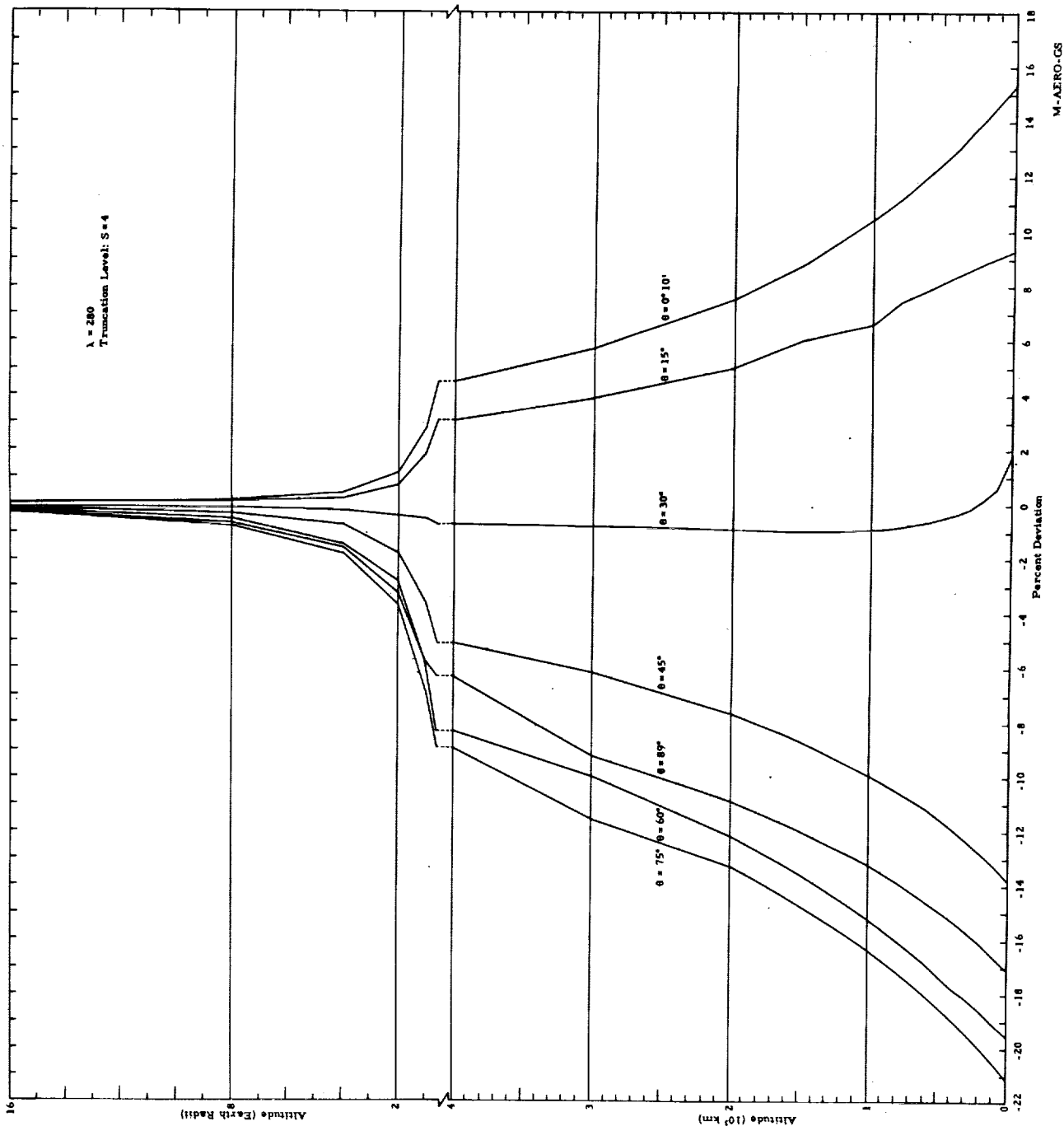
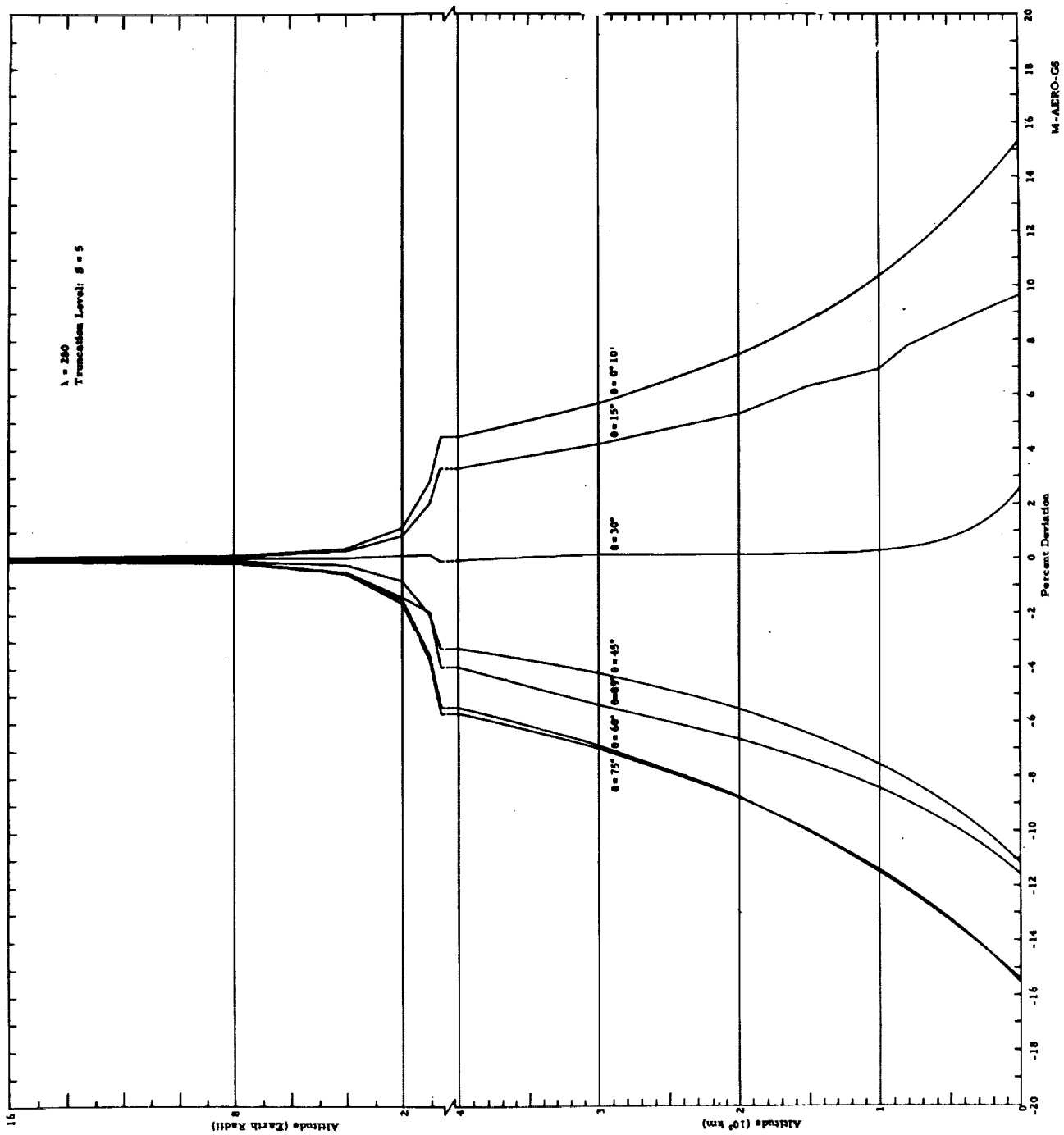


Fig. 13.d. Percent Truncation Levels at Various Colatitudes for $S = 4$

Fig. 13. a. Percent Truncation Levels at Various Colatitudes for $S = 5$

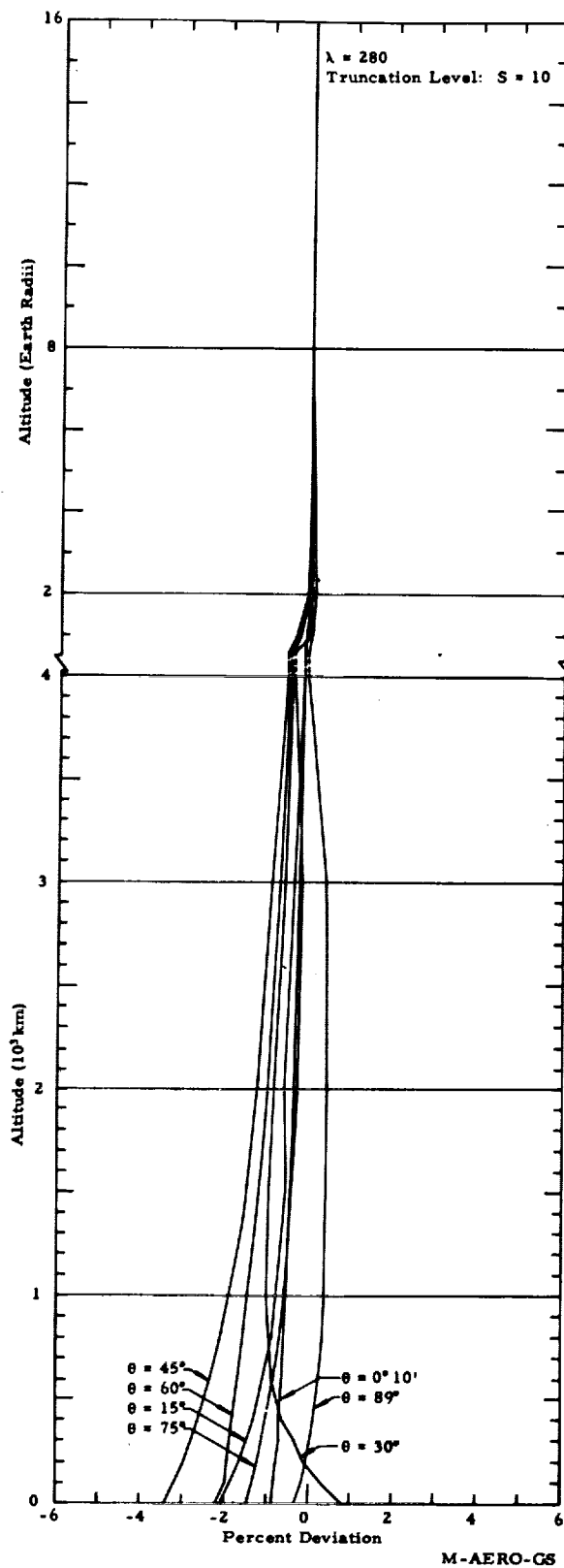


Fig. 13.f. Percent Truncation Levels at Various Colatitudes for $S = 10$

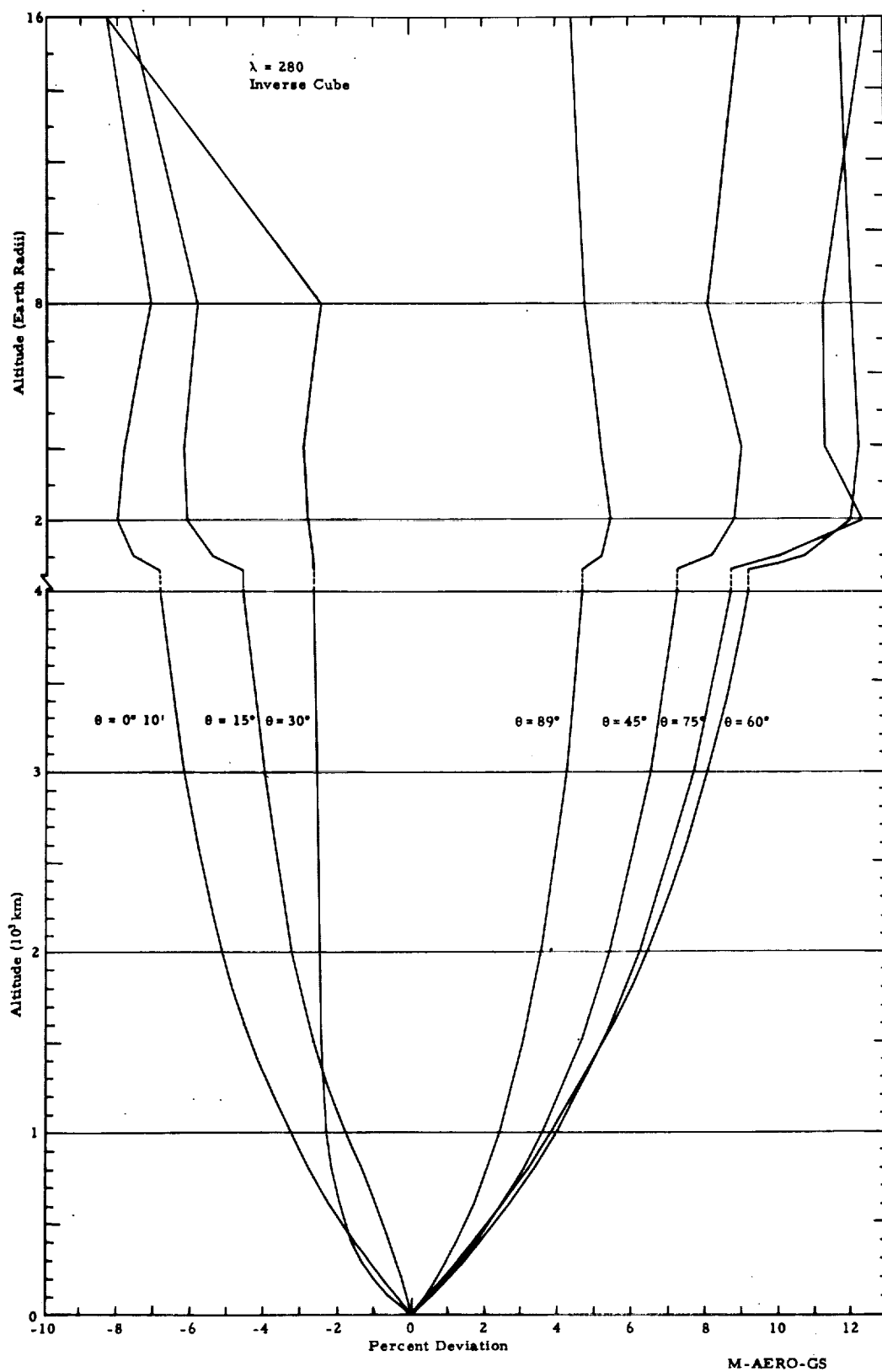


Fig. 14. Percent Deviations at Various Colatitudes of the Geomagnetic Field Computed With the Inverse Cube Relation from that Computed for $S = 296$

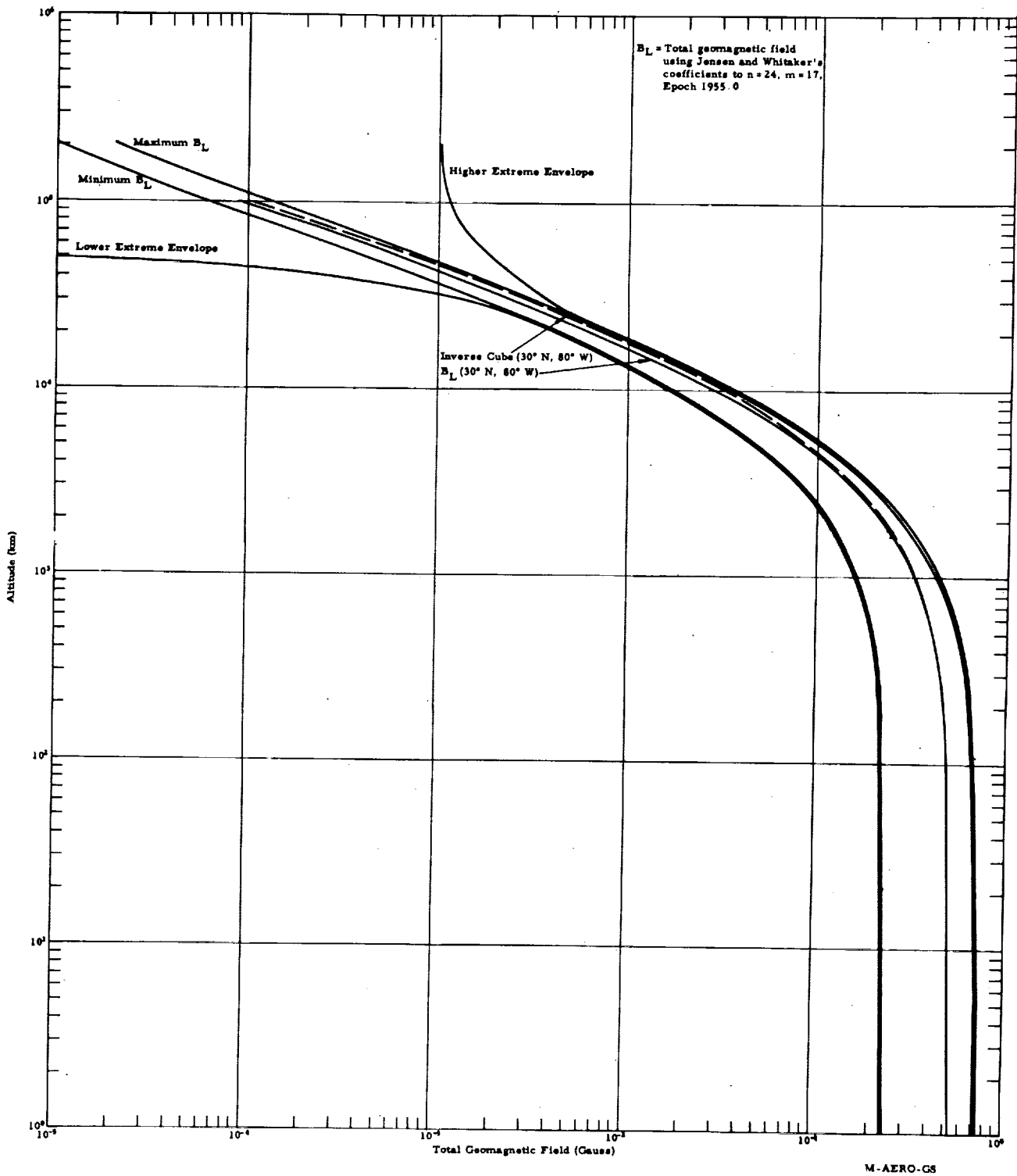


Fig. 16. b. Mean and Extreme Geomagnetic Field Curves for Epoch 1955.0

REFERENCES

1. Oxford, W. S., "The Interaction Between the Solar Wind and the Earth's Magnetosphere," *Journal of Geophysical Research*, Vol. 67, No. 10, 3791-3796, September 1962.
2. Sprieter, J. R. and A. Y. Alksne, "On the Effect of a Ring Current on the Terminal Shape of the Geomagnetic Field," *Journal of Geophysical Research*, Vol. 67, No. 6, 2193-2206, June 1962.
3. Chapman, S. and J. Bartels, "Geomagnetism," Volume II, Oxford University Press, New York, 1951, p. 626, p. 639.
4. Schmidt, A., "Tafeln der normierten Kugelfunktionen und ihrer Ableitung neben den Logarithmen dieser Zahlen sowie Formeln zur Entwicklung nach Kugelfunktionen." Gotha, Engelhard-Reyher Verlag, 1935.
5. Vestine, E. H., "On Variations of the Geomagnetic Field, Fluid Motions, and the Rate of the Earth's Rotation," *Journal of Geophysical Research*, Vol. 58, No. 2, p. 127-145, June 1953.
6. Jones, H. S. and P. J. Melotte, "The Harmonic Analysis of the Earth's Magnetic Field, for Epoch 1942," *Monthly Notices of the Royal Astronomical Society, Geophysical Supplement*, Vol. 6, No. 7, p. 409-430, June 1953.
7. Dyson, F. and H. Furner, "The Earth's Magnetic Potential," *Monthly Notices of the Royal Astronomical Society, Geophysical Supplement*, Vol. 1, No. 76, p. 76-88, May 1923.
8. Fanselau, G. and H. Kautzleben, "Die Analytische Darstellung des Geomagnetischen Felds," *Geofisica Pura E Applicata*, Milano, Vol. 41, p. 33-72, 1958.
9. Finch, H. F. and B. R. Leaton, "The Earth's Main Magnetic Field Epoch 1955.0," *Monthly Notices of the Royal Astronomical Society, Geophysics Supplement*, Vol. 7, No. 6, p. 314-317, 1957.

REFERENCES (CONTD)

10. Cain, J. C. et al., "Measurements of the Geomagnetic Field by the Vanguard III Satellite," NASA Technical Note D-1418, October 1962.
11. Beard, D. B. and E. B. Jenkins, "The Magnetic Effects of Magnetosphere Surface Currents," Journal of Geophysical Research, Vol. 67, No. 9, p. 3361-3368, August 1962.
12. Heppner, J. P., N. F. Ness, C. S. Scarce, and T. L. Shillman, "Explorer X Magnetic Field Measurements," X-611-62-125.

APPROVAL

MTP-AERO-63-60

AN EVALUATION OF VARIOUS GEOMAGNETIC
FIELD EQUATIONS

Harold C. Euler and Peter E. Wasko

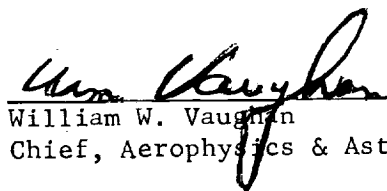
The information in this report has been reviewed for security classification. Review of any information concerning Department of Defense or Atomic Energy Commission programs has been made by the MSFC Security Classification Officer. This report, in its entirety, has been determined to be unclassified.



H. Euler
Aerospace Technologist, M-AERO-G



Robert E. Smith
Chief, Space Environment Section, M-AERO-GS



William W. Vaughan
Chief, Aerophysics & Astrophysics Branch, M-AERO-G



E. D. Geissler
Director, Aeroballistics Division, M-AERO-DIR

DISTRIBUTION

INTERNAL

M-DEP-R&D

M-FPO-DIR

M-SPA-DIR

M-ASTR

Director

Mr. F. Digesu

Mr. J. Boehm

M-COMP

Director

Mr. J. Armstrong

M-P&VE-DIR

M-RP

Director

Mr. G. Heller

Dr. W. Johnson (2)

Dr. R. Shelton

Mr. A. Thompson

M-LVOD-DIR

M-AERO

Director - - - - - M-AERO-DIR

Mr. O. C. Jean - - - - M-AERO-PS

Dr. R. F. Hoelker - - - M-AERO-P

Mr. P. J. de Fries - - - M-AERO-S

Mr. W. K. Dahm - - - - M-AERO-A (2)

Mr. H. J. Horn - - - - M-AERO-D (2)

Mr. O. C. Holderer - - - M-AERO-E

Dr. F. Speer - - - - - M-AERO-F

Mr. H. F. Kurtz - - - - M-AERO-FO

Mr. W. Murphree - - - - M-AERO-TS

Dr. W. Heybey - - - - - M-AERO-TS

Dr. H. Sperling - - - - M-AERO-TS

Mr. W. W. Vaughan - - - M-AERO-G

Mr. C. Dalton - - - - - M-AERO-G

Mr. J. Scoggins - - - - M-AERO-G

Mr. O. Smith - - - - - M-AERO-GT

Mr. R. Smith - - - - - M-AERO-GS

Mr. H. Euler - - - - - M-AERO-GS (10)

Mr. W. Roberts - - - - - M-AERO-GS

M-MS-IP

M-MS-IPL (8)

M-MS-H

M-HME-P

M-PAT

DISTRIBUTION

EXTERNAL

Mr. Ralph W. Murray, SWRFM
Physics Division
Research Directorate
Air Force Special Weapons Center
Air Force Systems Command
U. S. Air Force
Kirkland Air Force Base, N. M.

NASA
Manned Spacecraft Center
Houston, Texas
Attn: Director
Chief, Space Environment Division
Technical Library

NASA
Lewis Research Center
Cleveland, Ohio
Attn: Technical Library

NASA
Ames Research Center
Moffett Field, California
Attn: Technical Library

NASA
Goddard Space Flight Center
Greenbelt, Maryland
Attn: Dr. J. P. Heppner,
Magnetic Field Section, Fields & Particles Br.,
Space Sciences Division
Technical Library

NASA
Langley Research Center
Langley Field, Virginia
Attn: Mr. Edward W. Leyhe
Technical Library

DISTRIBUTION

EXTERNAL (Cont'd)

NASA
Launch Operations Center
Cocoa Beach, Florida
Attn: Director

NASA
Jet Propulsion Laboratory
4800 Oak Grove Drive
Pasadena, California
Attn: Dr. Conway Synder

Air Force Cambridge Research Laboratories
L. G. Hanscom Field
Bedford, Massachusetts
Attn: Technical Library

Mr. Peter E. Wasko, A2-260
Physics/Thermodynamics Section
Missile & Space Systems Division
Douglas Aircraft Company, Inc.
Santa Monica, California

Scientific and Technical Information Facility (2)
ATTN: NASA Representative (S-AK/RKT)
P. O. Box 5700
Bethesda, Maryland